The evolution of dependence and cohesion in incipient endosymbioses

Gaurav S. Athreya[1,2,3]✉, **Peter Czuppon**[4], **and Chaitanya S Gokhale**[1,3]

[1]Research Group for Theoretical Models of Eco-evolutionary Dynamics, Department of Theoretical Biology, , Max Planck Institute for Evolutionary Biology, August Thienemann Straße, Plön 24306, Germany
[2]Indian Institute of Science Education and Research, Pune, India
[3]Institute of Organismic and Molecular Evolution, University of Mainz, 55128 Mainz, Germany
[4]Institute for Evolution and Biodiversity, University of Münster, Münster, Germany
[5]Center for Computational and Theoretical Biology, University of Würzburg, Klara-Oppenheimer Weg 32, 97074, Würzburg, Germany

Eukaryogenesis is the prototypical example of an egalitarian evolutionary transition in individuality, and endosymbiosis, more generally, is central to the origins of many complex biological systems. Why do only some symbioses undergo such a transition, and how does the host-symbiont relationship change during this process? Here, we characterise endosymbiosis by two emergent collective-level properties: host and symbiont survival as a collective ("mutual dependence") and the level of synchronised reproduction ("reproductive cohesion"). Using adaptive dynamics, we study the evolution of the traits underlying these properties. First, by adding a carrying capacity for the collective population – a realism omitted in previous models – we find novel reasons why complete dependence or cohesion might not evolve, thus providing further theoretical support for the rarity of transitions in individuality. Second, our model suggests that asymmetries in evolutionary outcomes of hosts and symbionts can be explained by a difference in their population growth parameters, coupled with their shared fate when in a collective. Lastly, we show that during the early stages of an endosymbiosis, even if investments in dependence and cohesion are uncorrelated, mutual dependence arises faster than reproductive cohesion. Our results hence shed light on three aspects of endosymbiosis: coevolution between the host and symbiont, coevolution between dependence and cohesion, and ultimately on the opportunity of undergoing an evolutionary transition. Connecting to ecological factors, this work uncovers fundamental properties of endosymbioses, providing a clear way forward for theoretical and empirical investigations.

major evolutionary transitions | obligacy | mitochondria | microbiome | adaptive dynamics | Red King effect

Correspondence: *gathreya@uni-mainz.de*

Introduction

Endosymbiosis is a phenomenon of central importance in evolutionary biology, leading to the origin of eukaryotes and several astonishing long-term associations between different species. It is the prototypical example of an egalitarian transition in individuality: initially, autonomous and unrelated entities – the host and symbiont – come together to give rise to a more complex, integrated entity (1–4). The origin of endosymbiosis is not only a marked evolutionary transition but also a characteristic energy transition (5). Arguably, access to more energy processing via the endosymbionts set the stage for further evolutionary leaps such as multicellularity and beyond (6).

Endosymbionts are present in most life forms, even in unicellular prokaryotes (7, 8). Mitochondria and plastids have been famously shown to be endosymbionts arising from an ancient union between Archaeabacteria and an alphaproteobacterium (9–12). Many insects, such as the sap-sucking aphids, have been co-diversifying with their *Buchnera*, *Wigglesworthia*, and *Wolbachia* endosymbionts for millions of years (13–16). There are examples from diverse ecologies across the globe - methanogenic endosymbionts in anaerobic ciliates (17), nitrogen-fixing endosymbionts in the diatom *Rhopalodia* (18), consortia of chemosynthetic bacteria in gutless tubeworms (19), and cyanobacterial endosymbionts in sponges (20). New kinds of endosymbiotic associations continue being discovered, such as denitrifying endosymbionts in anaerobic ciliates (21). Despite this widespread prevalence, endosymbiosis and egalitarian evolutionary transitions are understudied relative to their fraternal counterparts, such as the evolution of multicellularity or eusociality (for which there exist many review or book-length treatments, e.g. (22, 23)). However, this point of view is slowly changing with the recent emergence of more studies on symbiosis (24–29).

In this work, we are interested in the relationship between the host and symbiont and how it evolves throughout an evolutionary transition in individuality. By a transition in individuality, we mean the emergence – from individuals of one or more species that can undergo evolution – of a higher-level entity that can itself undergo Darwinian evolution. Transitions where the lower-level individuals making up a collective are unrelated are called "egalitarian" (30). Some symbioses have undergone such a transition, whereas others have not. For example, proto-mitochondria and their ancestral hosts underwent a transition to form the modern eukaryotic cell (9). *Buchnera* endosymbionts are obligately dependent on their aphid hosts, vertically transmitted, and have small genomes (31). On the other hand, while the tubeworm *Riftia* is obligately dependent on its symbiont *Endoriftia*, the latter has a free-living stage, and is transmitted horizontally (32). Similarly, the bobtail squid *Euprymna scolopes* and its bioluminescent *Vibrio* symbiont are both facultative, and the symbiont is acquired horizontally every generation (33). What controls this difference in outcomes, and how is it impacted by the host's and symbiont's life-history traits? How do the properties of the collective co-evolve, and is there a differ-

DRAFT

ence between host and symbiont evolutionary trajectories? Such questions were introduced in the works of (24) and (28). These models emphasized different aspects of symbioses: (24) considered the evolution of an exploitative symbiont and showed that even unidirectional resource transfer can lead to an evolutionary transition. (28) considered a tradeoff between independent reproduction and host encounter rate, and showed that this can lead to evolutionary equilibria where the symbiont is facultatively dependent on its host. However, certain assumptions were made for analytical tractability, such as exponential population growth without any regulation for hosts, symbionts, or collectives (24) and ignoring the evolution of host traits, and letting collectives grow exponentially (28). In this study, we, too, make a new simplifying assumption (see the Model section, parameter d), but it allows us to relax many others and, in doing so, ask a variety of different questions about host-symbiont co-evolution with reasonable population dynamics.

To begin, we define a host-symbiont collective to be an obligate endosymbiosis if it exhibits three properties: (i) intracellular location of the symbiont; (ii) at least one of the host or symbiont is obligately dependent on this interaction; and (iii) the collective can reproduce synchronously, i.e. as a unit. Following (34), we use "symbiosis" to mean any sustained organismal interaction on the pathogenic-beneficial continuum. Synchronised collective reproduction, which is the target of our notion of "reproductive cohesion", is similar to, but stronger than, vertical symbiont transmission: we also include the requirement that the replication of the two partners is coupled, such as the coordination of mitochondrial fission and segregation with the cell cycle (although this is more complicated, see (35)). Importantly, synchronised reproduction endows the collective with a life cycle, previously proposed as the defining characteristic of an entity that can undergo an evolutionary transition (36). For example, our definition excludes gut microbiomes as there is no intracellular location or synchronised reproduction.

To study the conditions for the evolution of obligate endosymbiosis, we use evolutionary invasion analysis from the adaptive dynamics framework (37–40). This is a framework to study the long-term evolution by natural selection of traits that affect their bearer's ecological interactions. The evolutionary fate of new rare mutants is studied by determining if they can invade and fix in the population in which they arise. This analysis assumes the separation of ecological and evolutionary timescales: the ecological processes dictating the fate of a mutant ("natural selection") take place much faster than the timescale on which new host/symbiont mutants arise.

An eco-evolutionary model

We consider three populations – free-living hosts (H), free-living symbionts (S), and host-symbiont collectives (C). The primary process of interest is the evolution of the growth rates of these populations - we characterise obligate endosymbiosis by a positive growth rate for the collective and a zero growth rate for the free-living types.

Inspired by (25), we characterise a symbiosis by two emergent, collective-level quantities: the degree of host-symbiont mutual dependence and the degree of their reproductive cohesion (see Fig. 1). Mutual dependence is an aggregative measure of how well the two partners grow when free-living instead of when they are part of a collective; reproductive cohesion measures how often they reproduce synchronously instead of individually. The evolution of symbioses can thus be visualised as taking place in the plane of these two collective-level quantities. We say that an evolutionary transition in individuality occurs when there is complete mutual dependence and reproductive cohesion - the constituent individuals cannot live or reproduce without the other. We aim to understand the evolutionary trajectories in this dependence-cohesion plane. To study the joint evolution of the traits underlying dependence and cohesion, we use the method of evolutionary invasion analysis. The main object of interest is the invasion fitness of a mutant in the environment generated by a resident population. It is assumed in this framework that the ecological and evolutionary timescales can be separated, i.e., the (ecological) realisation of a mutant's fate takes place much faster compared to the (evolutionary) timescale on which the next mutant arises (37).

We formalise the ecological, i.e. population dynamics over short, mutation-free timescales as follows: Let f_H, f_S, f_C be the growth rates of the host, symbiont, and collective populations, respectively. Further, suppose the host and symbiont associate with and dissociate from each other at rates a and d, flowing into and out of the collective population. See Fig. 1(c) for a graphical representation of all possible events. The dynamics are given by:

$$\begin{aligned}
\dot{x}_H &= f_H x_H \left(1 - \frac{x_H}{K_H}\right) - a x_H x_S + d x_C, \\
\dot{x}_S &= f_S x_S \left(1 - \frac{x_S}{K_S}\right) - a x_H x_S + d x_C, \\
\dot{x}_C &= f_C x_C \left(1 - \frac{x_C}{K_C}\right) + a x_H x_S - d x_C
\end{aligned} \tag{1}$$

where K_i is the carrying capacity of population i. These dynamics are our default model, which we study extensively. To achieve some analytical results, we will also study this model with an infinite collective carrying capacity ($K_C \to \infty$). We also explore numerically different extensions, which we specify in the respective results sections.

The parameters of the population dynamical model above depend on the traits underlying dependence and cohesion. Consider first mutual dependence: we introduce the traits Ω_H and Ω_S, referred to hereafter as the "obligacy" of the host and symbiont, respectively (Fig. 1a). These are dimensionless numbers in $[0, 1]$ and denote the degree of dependence of the host and symbiont on the formation of the collectives. These traits formalise a tradeoff between individual (f_H, f_S) and collective reproduction rate f_C. To make explicit the co-localised nature of an endosymbiotic interaction, we assume that the benefits of endosymbiosis are only present when the organisms are part of the collective, implying, e.g. that the growth rates of the host population in isolation do not depend on the symbiont's investment (and vice versa).

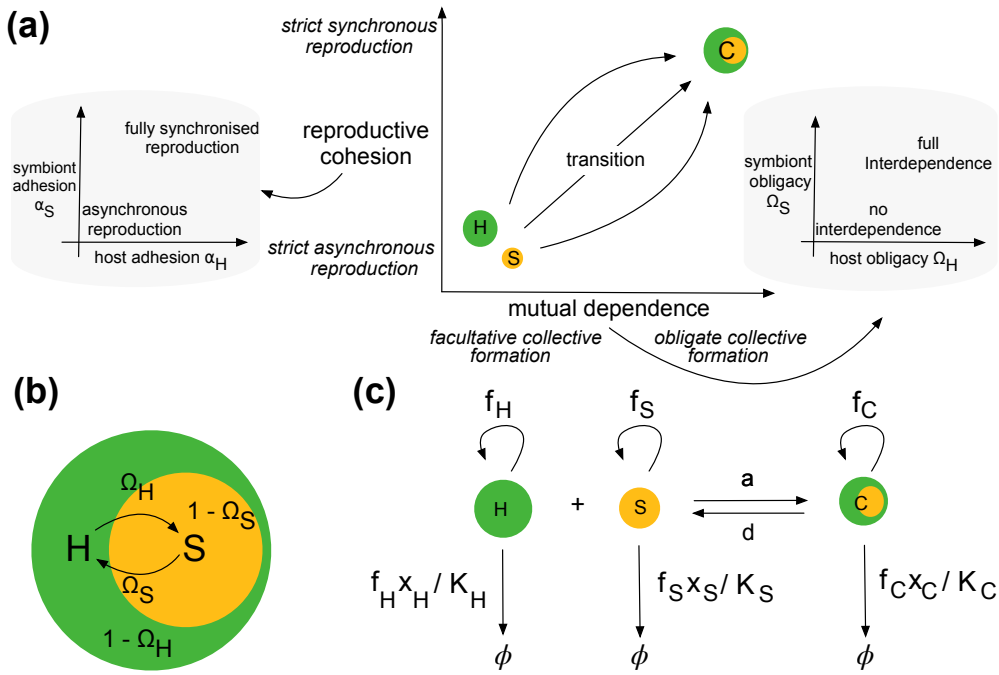

Fig. 1. (a) We conceptualise the trajectory of an evolutionary transition in the plane of two quantities - the reproductive cohesion of the lower-level individuals and the degree of mutual dependence between them. The adhesions α_H and α_S of the host and symbiont respectively control their investment in reproductive cohesion, i.e., the degree of synchronised reproduction. The obligacy Ω_i describes the investment of type i in growth as a collective. **(b)** On a microscopic scale, it is helpful to picture that there is – exclusively when they are both part of the collective – resource exchange between the host and symbiont. In this setting, the traits Ω_i control how much resource sharing the host/symbiont individuals are prone to. The trait α_i is more phenomenological and is most concretely connected to the magnitude of synchronised vs. asynchronised reproduction of species i. **(c)** The flows of the population dynamical model. All populations have a logistic growth rate corresponding e.g. to an intrinsic birth rate f_i and a density-dependent death rate $f_i x_i / K_i$. The host and symbiont associate and dissociate with rates a and d respectively.

With regards to reproductive cohesion, we introduce the traits α_H and α_S, hereafter referred to as the "adhesion" of the host and symbiont, respectively. These are also dimensionless in $[0,1]$, and a higher adhesion denotes a higher association rate a, lower dissociation d, and a higher propensity of synchronised birth f_C. These traits induce a tradeoff between processes favouring the formation of the collective and those favouring the individuals. The mathematical translation of these statements is in terms of the partial derivatives of f_i, a, d along the traits and is stated precisely in section §S.1.1 of the Supplementary Information (hereafter "SI"). The mapping of traits to population dynamical parameters that we will use for most of this work is

$$\begin{aligned} f_H(\Omega_H,\alpha_H,\Omega_S,\alpha_S) &= r_H(1-\Omega_H), \\ f_S(\Omega_H,\alpha_H,\Omega_S,\alpha_S) &= r_S(1-\Omega_S), \\ f_C(\Omega_H,\alpha_H,\Omega_S,\alpha_S) &= r_C\Omega_H\Omega_S\alpha_H\alpha_S, \\ d(\Omega_H,\alpha_H,\Omega_S,\alpha_S) &= d_0(1-\alpha_H\alpha_S), \\ a(\Omega_H,\alpha_H,\Omega_S,\alpha_S) &= a_0 \in \mathbb{R}_{\geq 0}. \end{aligned} \tag{2}$$

The parameters in our model are summarised in Table 1. In the Results section, we present analyses of a set of interconnected versions of the model set up thus far. We first study the evolution of dependence only – letting obligacies Ω_i evolve while the adhesions α_i stay constant – and then vice versa, i.e. cohesion only. We then introduce a simplified version of the population dynamical Eqs. 1 where the collective can grow exponentially; here we gain some analytical insights and study the joint evolution of obligacies and adhesions.

We assume a growth tradeoff: that any investment in independent reproduction from either host or symbiont comes at a cost to their contribution to the collective growth rate (and vice versa). Notice that in Eqs. S3, host independent growth rate f_H is maximum at $\Omega_H = 0$, decreases with increasing Ω_H, and is zero at $\Omega_H = 1$ (and identical for the symbiont). This tradeoff is inspired by the consideration that the selective pressures while in a collective and those while free-living are sufficiently contrasting that mutations have antagonistic effects in these two niches. For example, endosymbiont adaptation can be influenced by external pH levels or ambient amino acid availability, which are plausibly vastly different inside and outside the host. Similar statements about nutritional availability or pathogen defense can also be made for the pressures on host adaptation. Such tradeoffs have been observed in the squid-*Vibrio* symbiosis (41, 42), and in some experiments with *Bradyrhizobium* symbionts of plants (43) (see (44) for a more extensive discussion of growth tradeoffs). We are in this study interested primarily in mutualistic endosymbiosis, where increased investment from either partner increases the collective growth rate. The tradeoff above is a case where investment into collective growth is a priori difficult to emerge because of the linked cost to free-living growth. It is possible that only the symbiont experiences such a tradeoff or that there are mutations that only advantage the

collective or disadvantage the free-living host/symbiont; we do not consider these in our model.

To differentiate between the Ω and α trait pairs, it is useful to focus on an example such as a fig-wasp mutualism (reviewed in (45)). This association is an enmeshing of two life cycles – the fig tree depends on the wasp, the pollinator, and the wasp is dependent on the fig tree (the fruit, to be specific) to complete a part of its development. Therefore, the two species are highly dependent on each other, but they do not physically reproduce as a unit. Hence, here the obligacies Ω_i are high, but the adhesions α_i are not.

Evolutionary invasion analysis. To compute an arbitrary mutant's invasion fitness, we suppose a resident population is at ecological equilibrium, i.e., a stable steady state of the population dynamics (in our case Eq. (1)). The abundances at this steady state are computed numerically, unless mentioned otherwise. It is assumed that a mutant then arises, with trait value drawn from a symmetric probability distribution centred at the resident trait. The fate of this mutant is decided via its invasion fitness, i.e. the growth rate of a small number of mutants in the resident population (37). The mutant can invade if its invasion fitness is positive; if it is negative, the mutant goes to extinction (38, 46). This quantity is traditionally defined as the largest eigenvalue of the Jacobian of Eq. (1) when augmented for the presence of a mutant type. However, in our case, this quantity is not amenable to mathematical analysis, so we use the next-generation theorem, which gives an alternate characterisation of the same number (47, 48). We then use the canonical equation of adaptive dynamics (38) to study the macroscopic behaviour of long-term evolutionary trajectories (SI §S.4).

Results and Discussion

In the first subsection, we investigate the case where obligacies evolve independently of the adhesions and vice versa. In the second subsection, we analyse an extension of the model that includes within-collective birth and death rates. Then, in the third subsection, we study the relative importance of the collective population's growth rate and carrying capacity in deciding the course of evolution. Finally, in the last subsection, we study obligacy and adhesion coevolution in a model more amenable to analytics, which we derive by assuming an infinitely large collective carrying capacity in Eqs. 1.

It is challenging to analytically solve the system of Eqs. Eq. (1) to determine the fixed points and their stability. However, we determined computationally that for a wide range of parameter values, the dynamics converges to a stable fixed point over the evolutionary change in our traits of interest (see SI §S.2.1). Moreover, the values of the equilibrium population sizes increase or decrease gradually with the trait values, suggesting that there is a single internal fixed point. We will assume throughout that $K_S > K_H$ and $r_S > r_H$, i.e. the symbiont population has a higher carrying capacity and reaches it faster than the host. Consequently – on average over a given duration of time – more symbiont mutants arise than host mutants, and the symbiont trait hence has a higher rate of evolution (assuming, as we do, that the rate of mutation and the variance in the mutant trait distribution are the same for host and symbiont traits; see Eq. 4.12 in (38)).

Independent evolution of obligacies and adhesions. We begin by understanding the evolution of the obligacies when adhesions are kept constant, and vice versa. The mapping of obligacies to population dynamical parameters we use in Fig. 2, panels (a,b,c) is:

$$\begin{aligned} f_H(\Omega_H,\alpha_H,\Omega_S,\alpha_S) &= r_H(1-\Omega_H), \\ f_S(\Omega_H,\alpha_H,\Omega_S,\alpha_S) &= r_S(1-\Omega_S), \\ f_C(\Omega_H,\alpha_H,\Omega_S,\alpha_S) &= r_C\Omega_H\Omega_S, \end{aligned} \tag{3}$$

where we assume that the adhesions α_i are not under selection. The constants r_H, r_S, r_C set the scale of the parameters f_i; concretely, they can be understood as the intrinsic growth rates of the populations at either $\Omega_i = 0$ (for f_H and f_S), or when both obligacies are equal to 1 (for f_C). In panels (d,e,f) of Fig. 2, we assume obligacies to be constant and model the ecological consequences of a different adhesion via:

$$\begin{aligned} f_C(\Omega_H,\alpha_H,\Omega_S,\alpha_S) &= r_C\alpha_H\alpha_S \\ d(\Omega_H,\alpha_H,\Omega_S,\alpha_S) &= d_0(1-\alpha_H\alpha_S) \\ a(\Omega_H,\alpha_H,\Omega_S,\alpha_S) &= a_0 \in \mathbb{R}_{\geq 0} \end{aligned} \tag{4}$$

The constants r_C, d_0, a_0 are again the maximum values of the respective functions, and set the scale of variation.

Results are presented in Fig. 2. First consider the evolutionary trajectory of the obligacies $(\Omega_H(t), \Omega_S(t))$: the symbiont obligacy Ω_S reaches 1 first (denote this time by $t^*_{\Omega_S}$), and after this the selective pressure on Ω_H disappears, leading to stagnation in its value (Fig. 2a,b). This lack of selection after $\Omega_S = 1$ occurs because when $f_S = 0$ (no independent symbiont reproduction), the host and collective populations equilibrate to their carrying capacities irrespective of Ω_H; the symbiont population is sustained only through dissociation (see Eq. (1)). However, the symbiont has a higher equilibrium population size when $\Omega_S = 1$ than when $\Omega_S < 1$ due to the "backflow" from the dissociation of the collectives (see SI §S.2.1, or from Eq. (1)). The converse is valid for the host – its population size is not at the maximum possible over the trait space, while $\Omega_H < 1$. This is a counterintuitive result: the symbiont foregoes its ability to reproduce independently and has a higher equilibrium population size than its carrying capacity; the host now has a population size exactly equal to its carrying capacity (when it could be higher, i.e. at $\Omega_H = 1$), but retains its ability to reproduce independently (Fig. 2c). Indeed, it is better (in terms of abundance) for both the host and symbiont to give up independent reproduction and be sustained only through dissociation, but the faster-evolving population can do this first. The above argument can also be made analytically via the computation of the basic reproductive number of a mutant $R_0(\tilde{\Omega}_H, \Omega_H, \Omega_S)$, which denotes – roughly – the number of offspring left by a mutant host with obligacy $\tilde{\Omega}_H$ that arises in a resident population of hosts with obligacy Ω_H and symbionts with obligacy Ω_S (derived using the next-generation theorem, see SI §S.4.1). This quantity is

Table 1. A list of and associated information regarding all parameters named in our model.

Parameters	Description	Possible values	Comments
Ω_H, Ω_S	Host and symbiont obligacies	[0,1]	initially set to $(0,0)$
α_H, α_S	Host and symbiont adhesions	[0,1]	initially set to $(0,0)$
x_H, x_S, x_C	Population densities of host, symbiont, and collectives	$[0,\infty)$	equilibrium densities depend on trait values
f_H, f_S, f_C	Growth rates of H, S, and C populations	$[0,\infty)$	usually set such that $f_S > f_C > f_H$
K_H, K_S, K_C	Carrying capacities of H, S, and C populations	$[0,\infty)$	usually set such that $K_S > K_C > K_H$
a, d	Association and dissociation rates	$[0,\infty)$	initial $d >$ initial a
d_H, d_S	Within-collective mortality rates of host and symbionts	$[0,\infty)$	assumed to not depend on any traits
b_H, b_S	Within-collective birth rates of host and symbionts	$[0,\infty)$	assumed to not depend on any traits
r_H, r_S, r_C	Maximum values of f_H, f_S, f_C	$[0,\infty)$	Only relevant when Ω_i and/or α_i are evolving
d_0	Maximum value of d	$[0,\infty)$	Only relevant when α_i are evolving

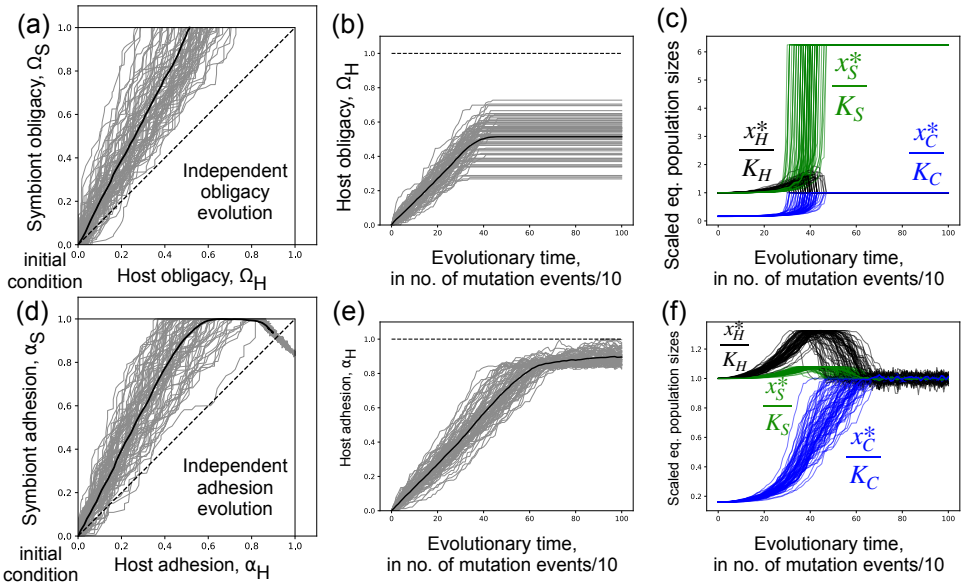

Fig. 2. Evolutionary dynamics of host and symbiont obligacies. All panels contain results of 75 independent stochastic simulations. **(a)** Symbiont obligacy evolves to 1, and then host obligacy is no longer under selection (see main text for an explanation). **(b)** Symbiont adhesion evolves to 1, and then host adhesion increases until a certain value. The traits together then vary along a neutral ridge around (1,1) (see main text for an explanation). **(c,d)** These panels show the evolutionary trajectory of the host trait, since it is here that the nontrivial outcomes take place. Ω_H plateaus at different values based on when the value of Ω_S reaches one. α_H increases up to a high value and stays close to it. **Parameter values**. Common for all: $K_H = 100, K_S = 200, K_C = 250, a_0 = 0.1$; for **(a)**: $r_H = 8, r_S = 20, r_C = 10, d = 50.0$; for **(b)** and **(c)**: $f_H = 8, f_S = 20, r_C = 10, d = 50$.

given by

$$R_0(\tilde{\Omega}_H, \Omega_H, \Omega_S) = \frac{\tilde{f}_H + \frac{dax_S^*}{(d-\tilde{f}_C)+\tilde{f}_C\frac{x_C^*}{K_C}}}{\tilde{f}_H\frac{x_H^*}{K_H} + ax_S^*} \quad \textbf{(5)}$$

where a star denotes that the value at equilibrium must be used. The R_0 is not maximally informative in our case since we cannot analytically solve for the equilibrium population abundances x_i^*. Nevertheless, it can be shown (see §S.4.1) that $R_0(\tilde{\Omega}_H, \Omega_H, 1) = 1$ for any combination $(\tilde{\Omega}_H, \Omega_H) \in (0,1]^2$ i.e. there is no fitness difference between any Ω_H mutants that arise in the background of $\Omega_S = 1$. A consequence of this result that cannot be captured by adaptive dynamics is that this model predicts the accumulation of neutral genetic variation in the host population at loci coding for obligacy.

Now consider the evolutionary trajectory of adhesions, presented in Fig. 2d,e. Symbiont adhesion α_S reaches 1 first while α_H is still smaller than 1, and then host adhesion increases until an evolutionarily stable strategy (ESS)

is reached. Trajectories then drift along a curve near (1,1). This ridge connects the states $(\Omega_H < 1, \Omega_S = 1)$ and $(\Omega_H = 1, \Omega_S < 1)$, and it is possible that a small proportion of trajectories eventually reaches $\Omega_H = 1$. The drift in Fig. 2d,e,f is what our model predicts of biological populations, however its source in this figure is different: accepting false positives when deciding the fate of mutants based on $R_0 > 1$, which arise due to floating point errors that we cannot entirely remove. All neutral mutations would have $R_0 = 1$, whereas we accept values only larger than a value that is infinitesimally larger than one to exclude such errors (see associated scripts for exact details).

Nevertheless, there are two facts to explain: that the traits increase and that there is a host-symbiont asymmetry in outcomes. Our observations can be explained by the variation in equilibrium population sizes as traits change (see SI §S.2.1 for heatmaps). Notably, (i) they increase along the adhesions α_i (and hence the traits themselves also increase); and (ii) they do so non-monotonically, with a local maximum in $x_i^*(\alpha_H, \alpha_S)$ occurring over a ridge in the interior of the $\alpha_H - \alpha_S$ space that surrounds the top right corner (1,1) (see Fig. §S.2.1). The first consequence is that any trajectory (α_H, α_S) must pass over this ridge to reach $(1,1)$. The symbiont adhesion can reach 1 before encountering this bump because of its faster rate of change, and the trajectory has to overcome it then while α_H is still less than 1. This is the source of the asymmetry: If both species have the same r and K, then the landscape of x_i^* is the same, but now the trajectory (α_H, α_S) hits the ridge when both adhesions are approximately equal and less than 1 (see SI §S.3.1). We suggest that the inflection point of this local maximum corresponds to the ESS, since decreasing population size (even locally) is disadvantageous, and such a mutant could not invade.

More proximately, an increased adhesion leads to modifications in two forces acting on host/symbiont population size via the term dx_C: (1) a decrease because fewer dissociations occur, but also (2) an increase because an increased adhesion increases f_C, and hence the collective population size. Since we begin with the intuitive scenario of high dissociation rate and zero synchronised growth, an initial increase in adhesion is beneficial, but this benefit is only up to a point, after which the decrease of d overpowers the increase due to f_C. This switch is the explanation for the presence of the intermediate ESS and the ridges in population size curves. This demonstrates that it is essential to consider not only intuitive parameters like f_H or f_S but also population size dynamics, which can strongly influence invasion fitness in this context.

The effect of within-collective mortality and reproduction. In our model, we have assumed so far that dissociation is perfect: all events producing free-living individuals from a collective give rise exactly to one host and one symbiont. However, it is likely that there is differential mortality for hosts and symbionts while they are in a collective or during dissociation. This would give rise to free-living hosts when the symbiont dies (at some rate d_S), and free-living symbionts with an analogous rate d_H. Further, hosts and symbionts, while in a collective, can also give birth to free-living hosts or symbionts. Suppose this takes place at rates b_H and b_S, respectively. The population dynamics is then described by

$$\begin{aligned}
\dot{x}_H &= f_H x_H \left(1 - \frac{x_H}{K_H}\right) - a x_H x_S + d x_C + (d_S + b_H) x_C, \\
\dot{x}_S &= f_S x_S \left(1 - \frac{x_S}{K_S}\right) - a x_H x_S + d x_C + (d_H + b_S) x_C, \\
\dot{x}_C &= f_C x_C \left(1 - \frac{x_C}{K_C}\right) + a x_H x_S - d x_C - (d_S + d_H) x_C.
\end{aligned} \tag{6}$$

The previous section then corresponds to, e.g. setting the rates $b_i = 0$ and $d_i = 0$ $i \in \{H, S\}$. The correspondence is slightly more general; one obtains Eqs. 1 whenever $b_i = d_j$ for all combinations of $i, j \in \{H, S\}$; with the caveat that the corresponding value of the dissociation rate would be higher, i.e. $d + b_i + d_j$.

We consider two scenarios: (i) differential mortality while in collective, but no within-collective reproduction ($d_H = d_S \neq 0, b_i = 0$ $i \in \{H, S\}$; Fig. 3 right), and (ii) within-collective H (or S) can give birth to free-living H (or S) but within-collective mortality is absent ($b_H = b_S \neq 0, d_i = 0$ $i \in \{H, S\}$; Fig. 3 left). For the sake of brevity, we do not consider the cases where $b_H \neq b_S$ or $d_H \neq d_S$, or where the within-collective birth and death rates are both greater than zero. However, the latter is not modelling a completely new phenomenon since d_i and b_j appear together as an aggregate coefficient of the collective abundance x_C in Eq. (S14). First, the adhesion trajectories (Fig. 3 right): there are no qualitative changes compared to the case when $d_i = b_i = 0$, the prediction that the adhesions increase and then hit a ridge of evolutionarily stable strategies is robust to the addition of the above within-collective rates. At higher shared values of d_i, the adhesions do not increase from initial values (see SI §S.3.4).

The evolution of obligacies, however, displays departures both when $d_i > 0$ or $b_i > 0$. When hosts or symbionts can die while in a collective but cannot give birth, the obligacies do not initially increase from (0,0) at all. However, if the obligacies are at a high enough initial value to begin with, the obligacies then increase as before, with the symbiont obligacy Ω_S reaching 1 first. This threshold initial value increases with the shared value of d_H and d_S, but above this value the dynamics proceed similarly to the earlier model (see SI §S.3.4), with one important difference: once $\Omega_S = 1$, the selective pressure on Ω_H does not disappear, instead now the host obligacy also increases to 1, leading to full mutual dependence. At the state $\Omega_H = \Omega_S = 1$, the equilibrium population abundances remain at steady, non-zero values in our case of $d_S = d_H$.

When hosts and symbionts can give birth while in a collective but cannot die, the outcome is again different: the obligacies directly increase from (0,0) without needing a threshold dependence, but once symbiont obligacy reaches 1, the host is under selection to now decrease its obligacy. This leads to a non-monotonic route to a one-sided mutualism, where the symbiont is completely dependent and the host not at all. In

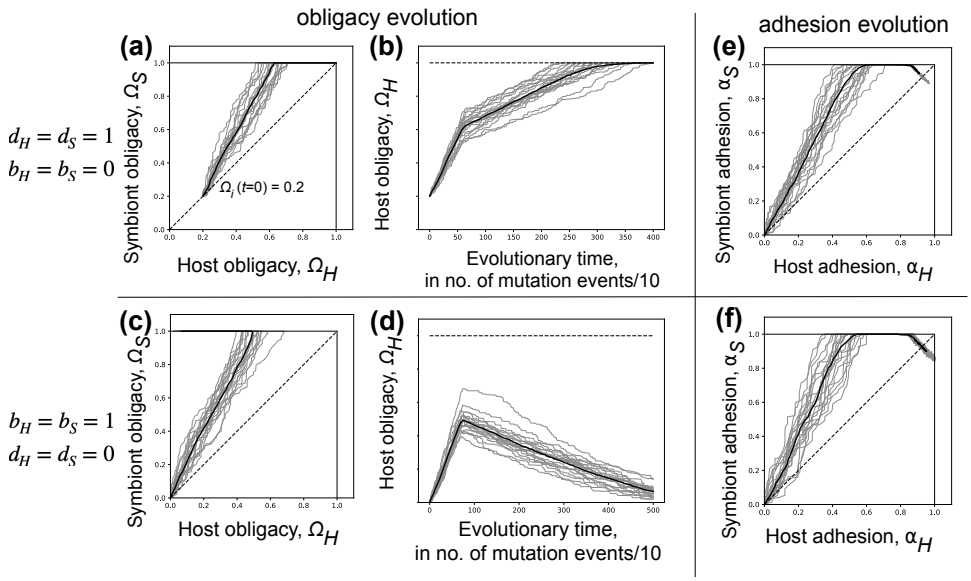

Fig. 3. Evolutionary dynamics of obligacies and adhesions when b_i and d_i are nonzero. All panels contain results of 20 independent stochastic simulations. **(a,b)** When $d_H = d_S > 0$, the initial obligacies must be above a threshold for them to further increase. Symbiont obligacy increases faster, and when Ω_S hits 1, host obligacy increases further upto 1. **(c,d)** When $b_H = b_S > 0$, dependence directly increases over time without a threshold minimum value that is necessary; when Ω_S hits 1, host obligacy now decreases to zero. **(e,f)** Qualitatively identical to adhesion evolution presented in Figure 2. **Parameter values**. Common for all: $K_H = 100, K_S = 200, K_C = 250, a_0 = 0.1$. Panels **(a,b,e)**: $d_H = d_S = 1, b_H = b_S = 0$. Panels **(c,d,f)**: $d_H = d_S = 0, b_H = b_S = 1$. Panels **(a,b,c,d)**: $r_H = 8, r_S = 20, r_C = 10, d = 50.0$. Panels **(e,f)**: $f_H = 8, f_S = 20, r_C = 10, d_0 = 50$.

the ultimate state of $\Omega_H = 0, \Omega_S = 1$, there is no fixed point possible for Eqs. S14; the symbiont goes extinct, while the host and collective populations blow up due to the birth rates. At higher shared values of b_i, the obligacies still increase, but host-symbiont symmetry in obligacies is reduced (see SI §S.3.4).

To explain the results above, we again appeal to the population sizes at equilibrium. It can be shown that, if $d_S + b_H = d_H + b_S$ (which is true in Fig. 3 by the parameters we have set), once $\Omega_S = 1$ (implying $f_S = 0$), the equilibrium abundances calculated from Eqs. S14 are given by the equations

$$\begin{aligned} x_H^* &= K_H, \\ x_C^* &= \left(1 + \frac{(b_S - d_S)}{f_C}\right) K_C, \\ x_S^* &= \frac{(d + d_H + b_S) x_C^*}{a x_H^*}. \end{aligned} \tag{7}$$

Dependence on Ω_i here enters through the f_C in x_C^*: when $b_S > d_S$, an increased host obligacy decreases collective abundance at equilibrium x_C^*, and when $b_S < d_S$, an increased host obligacy *increases* x_C^*. More generally, the form of x_C^* reflects that the forces driving the collective population away from its carrying capacity are b_S-produced free-living symbionts which form collectives via host association, and collectives leaving the compartment at rate d_S to form hosts. This suggests that even if the rates b_i and d_i are unequal, a case we have not tested here, the difference $b_S - d_S$ plays a central, if not solitary, role in deciding the outcome.

The inclusion of births and deaths of hosts and symbionts while in collective therefore affects two properties of the trajectory: initial increase of the obligacies, and what happens when $\Omega_S = 1$ is reached (see Table 2 for a summary of these effects). Including trait-dependence onto these within-collective rates would further complicate the picture since their values would become dynamic, and combinations of the above arguments might become necessary. We do not consider this possibility here, but some possible consequences are discussed in the Conclusions section. Having clarified the effects of the parameters b_i and d_i, we shall set them again to zero for the remaining sections to emphasize other predictions of this model.

Collective growth rate and collective carrying capacity have different effects on evolutionary outcomes. We have shown that dependence and cohesion can, in fact, increase under our assumptions, and that associating with a partner to form a collective is thus beneficial. However, this benefit is in terms of two independent (at least in our model) parameters - the collective population's growth rate r_C and its carrying capacity K_C. In this section, we are interested in which of these parameters is more important in determining the evolutionary outcome. We computed evolutionary trajectories for high and low values of the parameters r_C and K_C each – $r_C \in \{1, 40\}$ and $K_C \in \{10, 500\}$. At the low value of K_C, both obligacies and adhesions remained at their initial condition (0,0); at the high value of K_C, they evolved away from (0,0). The outcome was not influenced by the value of r_C. This shows that it is more important that the collective's equilibrium population size is high, no matter how much the mutant and resident differ in how fast they reach this size. We propose a cutoff for the threshold value of K_C in the following paragraphs.

Nevertheless, once K_C is high enough, its precise value can influence the ultimate values of adhesion, but not obligacy. Fig. 4 presents the results of evaluating the evolutionary tra-

Table 2. A summary of evolutionary outcomes for Ω_i and α_i depending on the rates of within-collective mortality and reproduction.

Scenario	Parameters	Consequences on $\Omega_i(t)$	Consequences on $\alpha_i(t)$
Perfect collective dissociation, no within-collective births or deaths	$d_H = 0$, $d_S = 0$ $b_H = b_S = 0$	both increase, host obligacy stagnates once symbiont completely obligate	increase, then drift along a ridge
Within-collective mortality, but no births	$d_H = d_S > 0$, $b_H = 0$, $b_S = 0$	both increase if initial obligacy high enough, ultimately both host and symbiont both become obligately dependent	increase, then drift along a ridge
Within-collective hosts can give birth to new hosts (similarly symbionts), but no within-collective deaths	$b_H = b_S > 0$ $d_H = 0$, $d_S = 0$	both increase without a threshold, ultimately symbiont becomes fully obligately whereas host completely independent	increase, then drift along a ridge
Within-collective birth and death rates are all equal	$b_H = b_S = d_H = d_H$	equivalent to setting $b_i = d_i = 0$, and increasing d, so there is no formal difference to the first row	

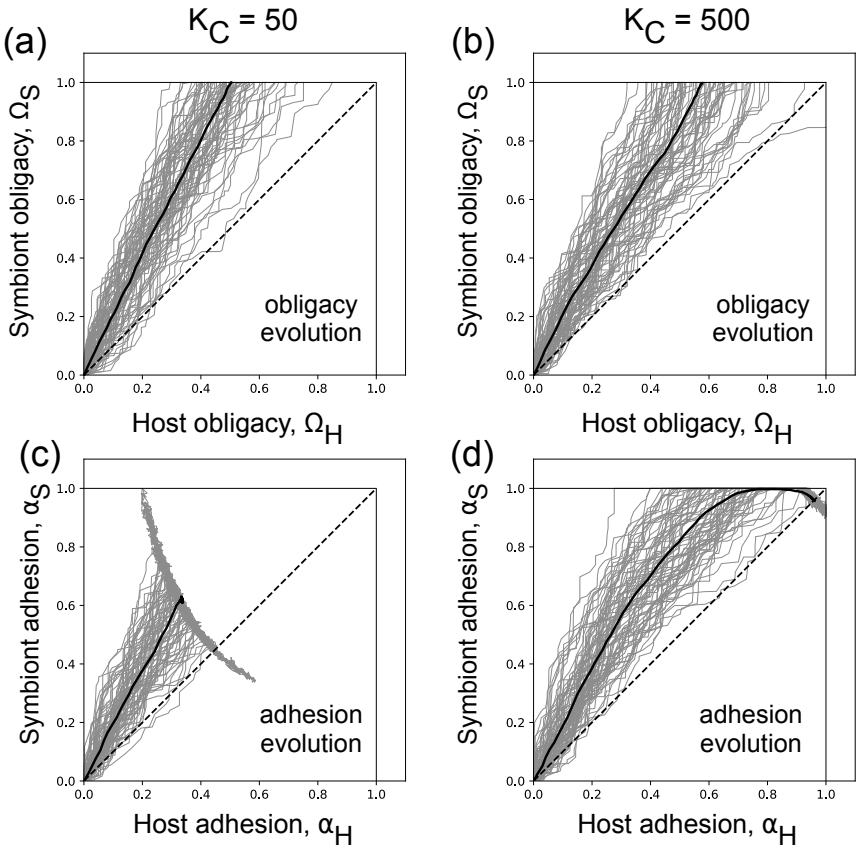

Fig. 4. Collective carrying capacity qualitatively and quantitatively affects ultimate trait values. Each panel contains the results of 75 independent simulation runs (in grey), with the average trajectory in solid black. Both values of $K_C = 50, 500$ in this figure are high enough to allow traits to increase from (0,0).$K_C = 10$ was not. When K_C is high enough, obligacies increase such that symbiont obligacy evolves to 1 and host obligacy subsequently is no longer under selection. Ultimate values of adhesion are affected by the precise values of K_C. The question of how high K_C must be is addressed in the main text. This outcome did not change between simulations run under low and high values of $r_C = 1$ and $r_C = 40$ respectively. **Parameter values**. $a_0 = 0.1, d = 50, r_H = 8, r_S = 20, r_C = 40, K_H = 100, K_S = 200$; r_C and K_C vary as indicated in the figure.

jectories of obligacies and adhesions at two values of the parameters K_C, both of which are high enough to allow traits to increase from (0,0) but quantitatively different.

Obligacy evolution is not affected by the value of K_C. This is in line with our intuition developed in the previous sections – the defining event in an increasing obligacy trajectory is the location of its arrival at the unit square's boundary, and this cannot be affected by K_C, a parameter that does not bias trajectories preferentially towards hosts or symbionts. The bias $\Omega_S > \Omega_H$ does indeed persist, induced by the difference

in host and symbiont population growth parameters – something we did not manipulate for these tests.

Adhesion trajectories, however, are affected by the precise value of K_C. This is because the important event here is the trajectory's arrival at the neutral ridge of ESSs described in the previous section. The presence of this ridge is explained by the non-monotonically varying benefit that dissociation of collectives provides to independent host and symbiont populations. Therefore, it is intuitive that the ridge's location is affected by K_C, a parameter that strongly sets the equilibrium abundance of collectives. At lower K_C, the relative number of collectives is lower and hence dissociation becomes non-beneficial at relatively lower values of the adhesions and hence relatively higher values of the effective dissociation rate $d_0(1-\alpha_H\alpha_S)$.

Note that the ridge when $K_C = 50$ also prevents the adhesions from reaching maximum values even for the symbiont (despite the bias $\alpha_S > \alpha_H$ persisting for identical reasons as above). When the carrying capacity K_C is very high (see SI §S.3.3), this ridge is extremely close to (1,1) and the adhesions effectively reach their maximum values. The slight movements around $\Omega_H(t^*_{\Omega_S})$ and the drift of adhesions along the ridge are artefacts of floating-point errors as before and can be ignored; we refrain from finding an involved artificial way to remove these since their origin is provably clear (see previous sections).

The $r-K$ difference in importance is also reflected in the variation of the equilibrium population sizes as traits evolve (SI §S.2.1). The pattern of variation supports the claims we have made so far – it is not qualitatively affected by the value of r_C, but is so affected by changes in K_C. The ridge in population sizes can also be shown to be closer to (1,1) for higher K_C. This agrees with the intuition that the scale of the equilibrium population size x^*_C is set more strongly by K_C, with a smaller spread around it that is determined by other parameters. The maximum population size attained by the collective is its carrying capacity, and this takes place when at least one of $(\Omega_H, \Omega_S) = 1$, and when both $\alpha_H = \alpha_S = 1$. Our analysis suggests that the pattern of variation switches depending on which quantity is bigger - dK_C or aK_HK_S, i.e. outflow or inflow into the population i when $\Omega_i = 1$. In particular, when $\Omega_H = \Omega_S = 0$, population sizes equilibriate to $x^*_H = K_H, x^*_S = K_S$; when $\Omega_i = 1$ for $i = \{H,S\}$, then $x^*_i = \frac{dK_C}{aK_j}$ where j is the other species. This suggests a sufficient condition on how high K_C must be: if $K_C > \frac{aK_HK_S}{d}$, hosts and symbiont populations are incentivised to increase obligacy. We tested this by varying a and d to perturb the same threshold quantity, and the results support our claim (see SI section §S.3.2). These arguments are difficult to make fully explicit given intractable analytical results – a problem that we directly address in the next section.

Does mutual dependence evolve before or after reproductive cohesion?. To understand the co-evolution of both obligacies and adhesions across the host and symbiont, we introduce a simpler version of Model Eq. (1). The motivation is two-fold: first, it allows for analytical tractability, enabling better understanding of our model; second, it restricts focus to the early evolutionary dynamics, since the dynamics at the boundaries is strongly dependent on the parameters b_i and d_i. This simpler model assumes that the collective population exhibits unbounded exponential growth, i.e. that the carrying capacity is infinitely high. The "exponential model" will henceforth refer to the following system of ordinary differential equations:

$$\begin{aligned}\dot{x}_H &= f_H x_H\left(1-\frac{x_H}{K_H}\right) - a x_H x_S + d x_C,\\ \dot{x}_S &= f_S x_S\left(1-\frac{x_S}{K_S}\right) - a x_H x_S + d x_C,\\ \dot{x}_C &= f_C x_C + a x_H x_S - d x_C.\end{aligned} \tag{8}$$

Analogously, Eq. system Eq. (1) will now be referred to as the "logistic model" when necessary. One must keep in mind that comparisons to the logistic model of the previous sections can be made only when the traits Ω_i and α_i (and hence f_C, see the mapping Eq. (S3)) are of small value, since once f_C is high enough, the self-limitation term $-f_C x_C/K_C$ of the logistic growth rate becomes relevant. The formation of the collective can here be formally shown to be comparable to a mutualism between the host and symbiont, see SI §S.1.2. Many statements can now be made regarding the existence, feasibility, and stability of population dynamical equilibria. The precise statements are relegated to the SI, in §S.2.2 and §S.4.2; however, the important features are that there is only one stable internal fixed point, which is feasible when the dissociation rate d is high enough to counteract the exponential growth of the collective. This is also borne out in the evolutionary dynamics of Ω_i and α_i under the exponential model (see §S.4.2); the traits increase until a point, and much before either has reached its maximum value, the collective's reproduction is so strong that no ecological equilibrium exists and the collective population blows up to infinity. Analogous to Eq. (5), an R_0 value can also be calculated here, and it is very close in functional form to the R_0 under the logistic model. In particular, it is given by

$$R_{0,exp}(\tilde{\Omega}_H, \Omega_H, \Omega_S) = \frac{\tilde{f}_H + \frac{dax^*_S}{(d-f_C)}}{\tilde{f}_H \frac{x^*_H}{K_H} + ax^*_S} \tag{9}$$

and is exactly the result of taking $K_C \to \infty$ in the logistic R_0 (see Eq. (5)). This shows that the evolutionary dynamics captured by the exponential model are, at early trait values, truly comparable to the logistic model Eq. (1). In fact, one can go further here, and derive an exact invasion criterion – suppose a host mutant arises with obligacy $\widetilde{\Omega}_H$ and adhesion $\widetilde{\alpha}_H$. We show (§S.4.2) that this mutant will invade if and only if

$$\frac{\widetilde{f}_H}{\widetilde{a}}\left(1-\frac{\widetilde{d}}{\widetilde{f}_C}\right) > \frac{f_H}{a}\left(1-\frac{d}{f_C}\right). \tag{10}$$

where quantities with a tilde ($\sim$) are associated to the mutant. Since the host and symbiont are in our model identical

in everything but the label we impose on them, an analogous criterion exists for the fate of a symbiont mutant. This criterion is "separable" into two quantities of the same functional form, each depending only on either the mutant or the resident. This implies that over the course of successive mutations, this underlying quantity is maximised. The existence of such an optimisation principle (49) also means that there can never be evolutionary branching in our traits at these early times, see §S.4.4. Finally, using the constraints we set up in the Model section and §S.1.1, it can also be shown that all four traits $\Omega_H, \Omega_S, \alpha_H, \alpha_S$ must monotonically increase over evolutionary time.

To study dependence-cohesion coevolution, we again consider the mapping in Eq. (S3); results of the simulations are shown in Fig. 5. We represent the degree of dependence between the host and symbiont by the product $\Omega_H \Omega_S$ of their obligacies, and the degree of reproductive cohesion by $\alpha_H \alpha_S$[1]. These results show two important facts. First, for both the host and symbiont, it is adaptive to evolve such that $\Omega_i > \alpha_i$, i.e. being more obligate than cohesive, results from natural selection. Focusing on $\Omega_H \Omega_S$ and $\alpha_H \alpha_S$, one concludes that evolutionary trajectories are biased toward more mutual dependence than reproductive cohesion. This is a central result. It shows that, over time, we expect that a host-symbiont collective evolves such that the partners are closer to complete mutual dependence than to reproducing synchronously.

Fundamentally, this is because the functional effects of the pairs of traits are different. Recall that both trait pairs increase because of the better growth of the collective. However, there is a difference between them: independent growth of type i ($\in \{H, S\}$) is a function only of Ω_i, whereas the effect of the α_i occurs only in "coordination" with both species since dissociation is a function of the product of α_H and α_S (see Eq. (S3)). Therefore, an increase in Ω_i has a higher functional effect (in increasing the invasion fitness) than the same increase in α_i, since the latter's effect is damped by the other adhesion as well (since $\alpha_i \in [0, 1]$). See SI §S.4.5 for a more comprehensive explanation via other functional form choices.

This result is robust to the choice of parameter values, different generation times, additive (instead of multiplicative) effect of the individual traits on the collective, etc. (SI Fig. S.14). The bias persists, and mutual dependence evolves faster than reproductive cohesion. This strongly suggests that endosymbioses in nature are more likely to be mutually dependent than cohesive.

Conclusions and conjectures

Endosymbiosis and the advances in complexity it made possible are astonishing. An endosymbiotic association led to eukaryotes and many other intricate associations between unrelated individuals. In this study, we endeavour to give a precise view of endosymbiosis as an egalitarian evolutionary transition in individuality and study the effect of some essential ecological factors on its origins.

We study two significant characteristics of an endosymbiotic collective undergoing an evolutionary transition - the reproductive cohesion of the host and symbiont (affected by host and symbiont adhesion, α_H and α_S), and the level of mutual dependence between them (obligacy, Ω_H and Ω_S). Our model shows that when obligacies evolve independently, one expects the symbiont obligacy to increase to its maximum value first, which can lead to the host obligacy being under selection to either increase, decrease, or stay constant under different ecological scenarios. This might explain the diversity in dependence outcomes that we see in nature, and we identify the two parameters in our model, b_i and d_i ($i = H, S$), that control this outcome. The adhesions also increase (with symbiont adhesion reaching high values first), ultimately leading to the accumulation of neutral variation due to drift of the evolutionary trajectory along a line of evolutionarily stable strategies. The final value of the adhesions depends on the collective carrying capacity. Second, we show that host-symbiont asymmetries in evolutionary outcomes arise due to differences in their population growth rates and carrying capacities. Lastly, we show that at early evolutionary times, the density of permitted evolutionary trajectories in the dependence-cohesion plane is not uniform: when Ω_i and α_i co-evolve, both species evolve to be more obligate than adhesive, irrespective of the rate of these traits' evolution.

Our work highlights the importance of considering differences between host and symbiont population growth parameters. That the symbiont trait (either obligacy or adhesion) increases faster than its host counterpart is due to the symbiont's larger population size and hence faster rate of evolution: an instantiation of the Red King effect (50, 51) – such a bias must be expected when host and symbiont interests are aligned, and defection (lower Ω or α) leads to a lower payoff. In the original Red King effect, the interest-aligning mechanism is a mutualism – an ecological interaction. Our analysis shows that the collective's formation (and shared fate) is another fundamental, interest-aligning mechanism in evolutionary transitions. Further, this faster rate of evolution has qualitatively novel effects in our model: in the case of obligacy, the symbiont evolves to full obligacy first, which leads to conditions where the host obligacy can be under selection to increase, decrease, or neutrally drift. Our model predicts full dependence for the interaction partner with higher growth rate and carrying capacity, and parameter-dependent scenarios for the partner with lower growth rate and carrying capacity. There are at least two more qualitatively different routes to asymmetric investments: first, the growth tradeoffs $f_H(\Omega_H)$ and $f_S(\Omega_S)$ for host and symbiont investing in collective reproduction might be different, and might in nature take non-linear forms. The work of (52) suggests that this might have a qualitative impact: in their model, obligate exploitation can be observed over mutual dependence when the growth benefit of losing a costly function is accelerating in

[1] The multiplicative form here is connected to how they map to ecological parameters - a multiplicative effect of the Ω_i on collective reproduction f_C motivates the interpretation of $\Omega_H \Omega_S$ as the degree of mutual dependence as opposed to other potential measures such as $\Omega_H + \Omega_S$.

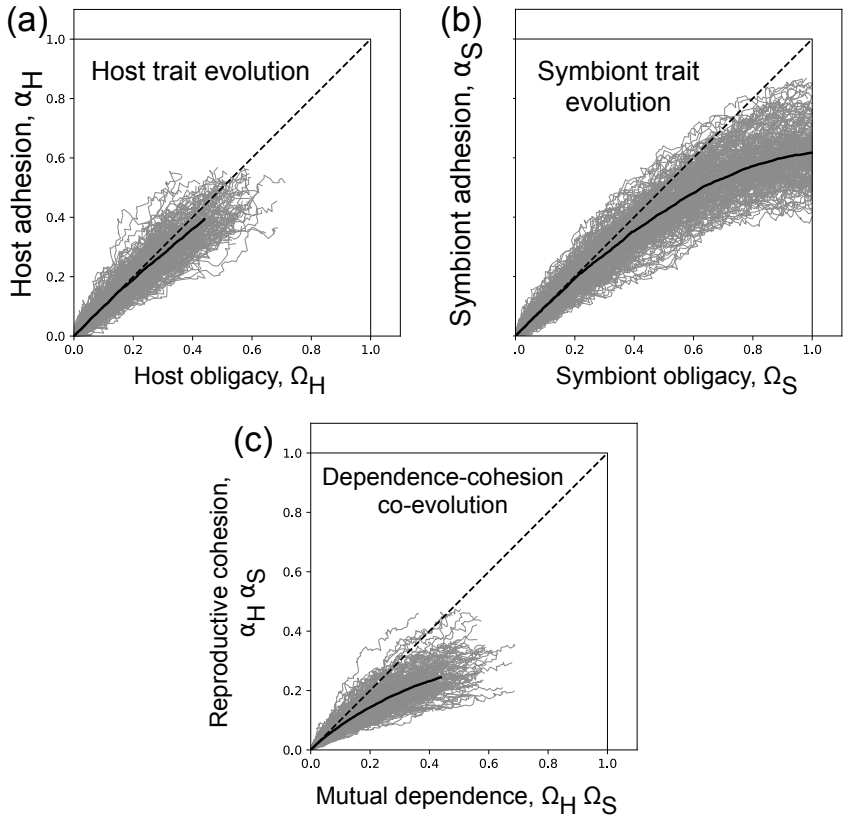

Fig. 5. Mutual dependence evolves before collective reproduction. Here we consider the co-evolution of the four traits Ω_H, α_H and Ω_S, α_S under the exponential model (Eqs. S6). **(a, b)** Both host and symbiont traits evolve such that, on average, $\Omega_i > \alpha_i$. Notice that symbiont evolution (panel **(b)**) shows that symbiont traits evolve to much higher values than host traits. **(c)** Given the individual evolutionary trajectories of the host and symbiont, one can collate information to obtain measures that describe the collective as a whole - the degree of mutual dependence is represented here by the product $\Omega_H \Omega_S$ and the degree of reproductive cohesion by $\alpha_H \alpha_S$. We observe that mutual dependence evolves faster than reproductive cohesion. The trajectories stop when they hit the feasibility bound; it is nontrivial to visualise its manifestation in this plane and is hence absent. **Parameter values**. $K_H = 100, K_S = 200, K_C = 500, a_0 = 0.1, r_H = 8, r_S = 20, r_C = 10, d_0 = 50.0$.

the amount of function lost. Further, we assumed that the within-collective reproduction and mortality rates are identical for host and symbiont. We assumed this for explanatory clarity, but it is almost certainly not true, and will give rise to new layers of asymmetry. Since these parameters are central to the evolutionary outcome, it is imperative in future work to measure them experimentally and characterise differences in their values. Developing this part of the theory might also help understand why current host-symbiont relationships are often biased towards the symbiont being much more obligate than the host. This is clearest in the evolution of tiny genomes in endosymbionts (31, 53, 54), and the ability to go through symbiont loss and replacements in some hosts (55). However, reductive genome evolution has also been shown to be driven by other mechanisms such as Muller's ratchet (56) or environment-induced redundancy (57–59), in addition to Red King-type effects. These latter effects are predicated on endosymbionts occurring within the hosts and not the other way around. Simple factors such as growth parameters and the nested structure of endosymbioses are therefore clearly important, and further work is required to delineate their consequences from that of complicated strategies such as partner choice/sanction or zero-determinant strategies (60, 61).

Another main aim was to understand why an evolutionary transition does not always take place. In this context, our model suggests the importance of the within-collective birth and death rates. They control model behaviour at two important timepoints: whether the obligacies initially increase, and what happens to the host obligacy once the symbiont becomes completely obligate. If within-collective births are stronger than deaths, (i) both obligacies increase initially, and (ii) host obligacy decreases to zero once the symbiont has become obligate. If the opposite is true, i.e. within-collective deaths are stronger than births, (i) the obligacies increase only above a certain threshold initial value, and (ii) the host becomes completely obligate once the symbiont has done so. Our model thus demonstrates that the evolutionary dynamics of dependence can impose strong constraints on the emergence of obligate endosymbioses. If the within-collective rates depend on the evolving traits Ω_i and α_i, it would allow for the situation where births are stronger than deaths initially (so both host and symbiont obligacies initially increase) and deaths are stronger than births later (and hence both become fully obligate). However, the rates may depend on different (combinations of) traits, and different dependence-structures of b_i, d_i on $\Omega_i, \alpha_i, i \in \{H, S\}$ might have different consequences. The values of b_i and d_i also need not be equal in the way that we have considered. Understanding the conse-

quences of these extensions constitutes, in our view, the next study necessary in this body of work. Lastly, full adhesions can be achieved only when the collective carrying capacity is very high; when it is lower, final adhesion values must be interpreted carefully since our model predicts drift over time and hence variability.

The prediction that dependence evolves faster than cohesion at early times can also be confronted with biological examples. Following the work of (25), we compiled a short, non-exhaustive list of well-studied endosymbioses (Table 3) where there is information on the level of vertical transmission (a proxy for reproductive cohesion) and the degree of mutual dependence. However, due to the qualitative nature of the data, the causal mechanics of the interactions are inconclusive. Some cases show direct connection to our theory: in the *Riftia-Endoriftia* endosymbiosis, there is high dependence but with horizontal transmission, others do not – the *Dictyostelium-Burkholderia* farming symbiosis is facultative from both sides and has a mixed mode of transmission (62). It is impossible to compare the degree of dependence and cohesion here. There is indirect evidence that mutual dependence is easier to evolve than reproductive cohesion, since it is widely observed empirically (63), understood well via e.g. the Black Queen effect (58), can evolve rapidly in an experiment (64), and in principle requires very few traits (52). On the other hand, few studies have precisely estimated quantities related to the level of vertical and horizontal transmission (65, 66). Further, it is not clear if there are genetic constraints that would lead to correlations in obligacy and adhesion – a strong enough correlation could shift in a new direction the bias towards codependence that we observe. On the theoretical side, an interesting extension of our model is to understand if the bias towards dependence that we see survives to later evolutionary times, when traits are closer to their final values. This study and its limitations thus highlight the need for a tighter connection between empirical work and theory and the requisite experiment where the complete evolutionary transition can be quantified. Nonetheless, taken as a null model, our study shows that an evolutionary transition in individuality is far from an inevitable outcome of the existence of a higher level of selection, suggesting that one might need to invoke different mechanisms to explain phenomena such as eukaryogenesis. While our model already allows for many of the scenarios that one would like to capture, many possible extensions exist that could improve the biological realism. Perhaps most importantly, we consider here the extreme case of the interaction becoming beneficial only in close proximity; one can also construct a model where interaction benefits are relevant even outside the collective. This would add Lotka-Volterra-type cross terms to the ecological dynamics captured by Eq. (1). Additionally, we set the collective's carrying capacity K_C to a constant value independent of host or symbiont traits, since we envision that the mechanism of benefit exchange underlying this endosymbiosis enables the colonisation of a new niche (broadly construed) and that this niche has an associated carrying capacity. Better or worse usage of the niche (via different trait values) does not guarantee a higher maximum occupancy, only a quicker rate of reaching it. Further, we consider that the collectives must always be formed by a fixed density of symbionts acquired together and only once, i.e. we do not consider symbiont growth inside a single host. The size of these symbiont blocks does not affect the dynamics of our model per se, and so one can think of a single symbiont inside each host without loss of generality. However, in reality, each host has a dynamically changing symbiont population, and successive symbiont acquisition events would allow, e.g. decreasing symbiont population sizes to be propped up by immigration, or to be qualitatively changed by mutualism or antagonism between different symbiont strains (see (29)). Selection on the host due to the interactions with multiple symbionts might add further selection pressures that lead to a transition. Lastly, we also do not consider that there might be competition between the independent types and the collective due to niche overlap. Relaxing each of these assumptions is a worthy and important direction for future work.

Statement of Authorship

Conceptualization: CSG, PC, GSA; Funding acquisition: CSG; Model development and analysis: GSA, PC, CSG; Computer scripts: GSA; Supervision: CSG; Writing (original draft): GSA; Writing (review & editing): PC, CSG, GSA.

Data and Code Availability

All data and simulation codes for generating the figures are available on Zenodo (https://doi.org/10.5281/zenodo.15533092).

ACKNOWLEDGEMENTS
GSA thanks the DST-INSPIRE programme of the Government of India for financial support and the Max Planck Society for supporting the research visit. CSG and GSA thank the Max Planck Society for generous funding. Ananda Shikhara Bhat and Vishwesha Guttal helped with the translation of the abstract. We are grateful to Erol Akçay and two anonymous reviewers for useful comments.

Bibliography

1. Eörs Szathmáry and John Maynard Smith. The major evolutionary transitions. *Nature*, 374 (6519):227–232, 1995.
2. David C. Queller. Relatedness and the fraternal major transitions. *Philosophical Transactions of the Royal Society of London. Series B: Biological Sciences*, 355(1403):1647–1655, November 2000. doi: 10.1098/rstb.2000.0727.
3. Eörs Szathmáry. Toward major evolutionary transitions theory 2.0. *Proceedings of the National Academy of Sciences USA*, 12(33):10104–10111, 2015.
4. Stuart A West, Roberta M Fisher, Andy Gardner, and E Toby Kiers. Major evolutionary transitions in individuality. *Proceedings of the National Academy of Sciences*, 112(33): 10112–10119, 2015.
5. Nick Lane and William Martin. The energetics of genome complexity. *Nature*, 467(7318): 929–934, 2010. ISSN 0028-0836. doi: 10.1038/nature09486.
6. N. Lane. *The Vital Question: Why is Life the Way it Is?* Profile Books, 2015. ISBN 9781781250365.
7. Daniel E. Wujek. Intracellular bacteria in the blue-green alga pleurocapsa minor. *Transactions of the American Microscopical Society*, 98(1):143, January 1979. doi: 10.2307/3225953.
8. Daniele Corsaro, Danielle Venditti, Maria Padula, and Marcello Valassina. Intracellular life. *Critical Reviews in Microbiology*, 25(1):39–79, January 1999. doi: 10.1080/10408419991299167.
9. Lynn Sagan. On the origin of mitosing cells. *Journal of Theoretical Biology*, 14(3):225–IN6, March 1967. doi: 10.1016/0022-5193(67)90079-3.
10. E. V. Koonin and N. Yutin. The dispersed archaeal eukaryome and the complex archaeal ancestor of eukaryotes. *Cold Spring Harbor Perspectives in Biology*, 6(4):a016188–a016188, April 2014. doi: 10.1101/cshperspect.a016188.
11. Joran Martijn, Julian Vosseberg, Lionel Guy, Pierre Offre, and Thijs J. G. Ettema. Deep mitochondrial origin outside the sampled alphaproteobacteria. *Nature*, 557(7703):101–105, April 2018. doi: 10.1038/s41586-018-0059-5.

Table 3. Dependence and cohesion information in some well-studied symbioses

Host-symbiont	Degree of dependence	Mode of transmission	References
Ancestral eukaryote host-protomitochondra, protoplastid	Mutually obligate	Vertical	(9)
Aphid-*Buchnera aphidicola*	Mutually obligate	Vertical	(16, 67–69)
Riftia-Endoriftia	Host obligate, symbiont facultative	Horizontal	(32, 70)
Dictyostelium discoideum-Burkholderia	Both facultative	Mixed	(62)
Squid-*Vibrio* (not intracellular)	Both facultative	Horizontal	(33)
Pea aphid-*Regiella*	Both facultative	Vertical, horizontal possible	(71, 72)
Legume-rhizobium	Both facultative	Horizontal	(73, 74)
Flatworm-*Riegeria*	Host obligate, symbiont dependence unclear	Vertical	(75)
Rhopalodia-nitrogen fixing *Cyanobacteria*	Mutually obligate	Vertical	(18)
Cicada-*C. sulcinia/hodgkinia*	Mutually obligate	Vertical	(76)

This table is a survey of symbioses for which there is nontrivial information of the degree of dependence and the mode of symbiont transmission (a proxy for reproductive cohesion), adapted from a similar table compiled by (25). The information present, however, is (i) qualitative, (ii) a snapshot of the current state. The current state does not carry information about the full evolutionary trajectory, and hence is insufficient to estimate the traits Ω_i and α_i. Therefore the available information does not allow us to confirm/refute the bias towards mutual dependence that our work predicts.

12. Lu Fan, Dingfeng Wu, Vadim Goremykin, Jing Xiao, Yanbing Xu, Sriram Garg, Chuanlun Zhang, William F. Martin, and Ruixin Zhu. Phylogenetic analyses with systematic taxon sampling show that mitochondria branch within alphaproteobacteria. *Nature Ecology & Evolution*, 4(9):1213–1219, July 2020. doi: 10.1038/s41559-020-1239-x.
13. Shuji Shigenobu, Hidemi Watanabe, Masahira Hattori, Yoshiyuki Sakaki, and Hajime Ishikawa. Genome sequence of the endocellular bacterial symbiont of aphids buchnera sp. APS. *Nature*, 407(6800):81–86, September 2000. doi: 10.1038/35024074.
14. Evelyn Zientz, Thomas Dandekar, and Roy Gross. Metabolic interdependence of obligate intracellular bacteria and their insect hosts. *Microbiology and Molecular Biology Reviews*, 68(4):745–770, December 2004. doi: 10.1128/mmbr.68.4.745-770.2004.
15. Martin Wu, Ling V Sun, Jessica Vamathevan, Markus Riegler, Robert Deboy, Jeremy C Brownlie, Elizabeth A McGraw, William Martin, Christian Esser, Nahal Ahmadinejad, Christian Wiegand, Ramana Madupu, Maureen J Beanan, Lauren M Brinkac, Sean C Daugherty, A. Scott Durkin, James F Kolonay, William C Nelson, Yasmin Mohamoud, Perris Lee, Kristi Berry, M. Brook Young, Teresa Utterback, Janice Weidman, William C Nierman, Ian T Paulsen, Karen E Nelson, Hervé Tettelin, Scott L O'Neill, and Jonathan A Eisen. Phylogenomics of the reproductive parasite wolbachia pipientis wMel: A streamlined genome overrun by mobile genetic elements. *PLoS Biology*, 2(3):e69, March 2004. doi: 10.1371/journal.pbio.0020069.
16. Allison K. Hansen and Nancy A. Moran. Aphid genome expression reveals host-symbiont cooperation in the production of amino acids. *Proceedings of the National Academy of Sciences*, 108(7):2849–2854, January 2011. doi: 10.1073/pnas.1013465108.
17. T. Martin Embley and Bland J. Finlay. Systematic and morphological diversity of endosymbiotic methanogens in anaerobic ciliates. *Antonie van Leeuwenhoek*, 64(3-4):261–271, 1994. doi: 10.1007/bf00873086.
18. Julia Prechtl, Christoph Kneip, Peter Lockhart, Klaus Wenderoth, and Uwe-G. Maier. Intracellular spheroid bodies of rhopalodia gibba have nitrogen-fixing apparatus of cyanobacterial origin. *Molecular Biology and Evolution*, 21(8):1477–1481, August 2004. doi: 10.1093/molbev/msh086.
19. Tanja Woyke, Hanno Teeling, Natalia N. Ivanova, Marcel Huntemann, Michael Richter, Frank Oliver Gloeckner, Dario Boffelli, Iain J. Anderson, Kerrie W. Barry, Harris J. Shapiro, Ernest Szeto, Nikos C. Kyrpides, Marc Mussmann, Rudolf Amann, Claudia Bergin, Caroline Ruehland, Edward M. Rubin, and Nicole Dubilier. Symbiosis insights through metagenomic analysis of a microbial consortium. *Nature*, 443(7114):950–955, September 2006. doi: 10.1038/nature05192.
20. R. W. Thacker. Impacts of shading on sponge-cyanobacteria symbioses: A comparison between host-specific and generalist associations. *Integrative and Comparative Biology*, 45 (2):369–376, April 2005. doi: 10.1093/icb/45.2.369.
21. Jon S. Graf, Sina Schorn, Katharina Kitzinger, Soeren Ahmerkamp, Christian Woehle, Bruno Huettel, Carsten J. Schubert, Marcel M. M. Kuypers, and Jana Milucka. Anaerobic endosymbiont generates energy for ciliate host by denitrification. *Nature*, 591(7850): 445–450, March 2021. doi: 10.1038/s41586-021-03297-6.
22. M.D. Herron, P.L. Conlin, and W.C. Ratcliff. *The Evolution of Multicellularity*. Evolutionary Cell Biology. CRC Press, 2022. ISBN 9781000542578.
23. Bert Hölldobler and E. O. Wilson. *The Superorganism: The Beauty, Elegance, and Strangeness of Insect Societies.* WW Norton, 2008.
24. Richard Law and Ulf Dieckmann. Symbiosis through exploitation and the merger of lineages in evolution. *Proceedings of the Royal Society of London. Series B: Biological Sciences*, 265 (1402):1245–1253, July 1998. doi: 10.1098/rspb.1998.0426.
25. Sylvie Estrela, Benjamin Kerr, and J Jeffrey Morris. Transitions in individuality through symbiosis. *Current opinion in microbiology*, 31:191–198, 2016.
26. István Zachar and Eörs Szathmáry. Breath-giving cooperation: critical review of origin of mitochondria hypotheses. *Biology Direct*, 12(1), August 2017. doi: 10.1186/s13062-017-0190-5.
27. István Zachar, András Szilágyi, Szabolcs Számadó, and Eörs Szathmáry. Farming the mitochondrial ancestor as a model of endosymbiotic establishment by natural selection. *Proceedings of the National Academy of Sciences*, 115(7), January 2018. doi: 10.1073/pnas.1718707115.
28. Phuong Linh Nguyen and Minus van Baalen. On the difficult evolutionary transition from the free-living lifestyle to obligate symbiosis. *PLOS ONE*, 15(7):e0235811, July 2020. ISSN 1932-6203. doi: 10.1371/journal.pone.0235811. Publisher: Public Library of Science.
29. Matishalin Patel and Stuart West. Microbial warfare and the evolution of symbiosis. *Biology Letters*, 18(12), December 2022. doi: 10.1098/rsbl.2022.0447.
30. J. Maynard Smith and E. Szathmáry. *The major transitions in evolution.* W. H. Freeman, Oxford, 1995.
31. Gordon M. Bennett and Nancy A. Moran. Heritable symbiosis: The advantages and perils of an evolutionary rabbit hole. *Proceedings of the National Academy of Sciences*, 112(33): 10169–10176, February 2015. doi: 10.1073/pnas.1421388112.
32. Andrea D. Nussbaumer, Charles R. Fisher, and Monika Bright. Horizontal endosymbiont transmission in hydrothermal vent tubeworms. *Nature*, 441(7091):345–348, May 2006. doi: 10.1038/nature04793.
33. Margaret J. McFall-Ngai. The importance of microbes in animal development: Lessons from the squid-vibrio symbiosis. *Annual Review of Microbiology*, 68(1):177–194, September 2014. doi: 10.1146/annurev-micro-091313-103654.
34. Patrick J. Keeling and John P. McCutcheon. Endosymbiosis: The feeling is not mutual. *Journal of Theoretical Biology*, 434:75–79, December 2017. doi: 10.1016/j.jtbi.2017.06.008.
35. Prashant Mishra and David C. Chan. Mitochondrial dynamics and inheritance during cell division, development and disease. *Nature Reviews Molecular Cell Biology*, 15(10):634–646, September 2014. doi: 10.1038/nrm3877.
36. J. van Gestel and C. E. Tarnita. On the origin of biological construction, with a focus on multicellularity. *Proceedings of the National Academy of Sciences USA*, 114(42):11018–11026, 2017.
37. J.A.J. Metz, R.M. Nisbet, and S.A.H. Geritz. How should we define 'fitness' for general ecological scenarios? *Trends in Ecology & Evolution*, 7(6):198–202, 1992.
38. U. Dieckmann and R. Law. The dynamical theory of coevolution: a derivation from stochastic ecological processes. *Journal of Mathematical Biology*, 34:579–612, 1996.
39. S. A. H. Geritz, É. Kisdi, G. Meszéna, and J. A. J. Metz. Evolutionarily singular strategies and the adaptive growth and branching of the evolutionary tree. *Evolutionary Ecology Research*, 12:35–57, 1998.
40. S. P. Otto and T. Day. *A Biologist's Guide to Mathematical Modeling in Ecology and Evolution.* Princeton University Press, Princeton, New Jersey, 2007.
41. M Sabrina Pankey, Randi L Foxall, Ian M Ster, Lauren A Perry, Brian M Schuster, Rachel A Donner, Matthew Coyle, Vaughn S Cooper, and Cheryl A Whistler. Host-selected mutations converging on a global regulator drive an adaptive leap towards symbiosis in bacteria. *eLife*, 6:e24414, apr 2017. ISSN 2050-084X. doi: 10.7554/eLife.24414.
42. Meagan Leah Cohen, Ekaterina Vadimovna Mashanova, Sveta Vivian Jagannathan, and William Soto. Adaptation to ph stress by vibrio fischeri can affect its symbiosis with the hawaiian bobtail squid (euprymna scolopes). *Microbiology*, 166(3):262–277, March 2020. ISSN 1465-2080. doi: 10.1099/mic.0.000884.
43. Joel L. Sachs, James E. Russell, and Amanda C. Hollowell. Evolutionary instability of symbiotic function in bradyrhizobium japonicum. *PLoS ONE*, 6(11):e26370, November 2011. ISSN 1932-6203. doi: 10.1371/journal.pone.0026370.
44. Michael A. Brockhurst, Duncan D. Cameron, and Andrew P. Beckerman. Fitness tradeoffs and the origins of endosymbiosis. *PLOS Biology*, 22(4):e3002580, April 2024. ISSN 1545-7885. doi: 10.1371/journal.pbio.3002580.
45. Edward Allen Herre, K. Charlotte Jandér, and Carlos Alberto Machado. Evolutionary ecology of figs and their associates: Recent progress and outstanding puzzles. *Annual Review of Ecology, Evolution, and Systematics*, 39(1):439–458, December 2008. doi: 10.1146/annurev.ecolsys.37.091305.110232.
46. Fabio Dercole and Sergio Rinaldi. *Analysis of Evolutionary Processes: The Adaptive Dynamics Approach and Its Applications.* Princeton University Press, 2008.
47. P. van den Driessche and James Watmough. Reproduction numbers and sub-threshold endemic equilibria for compartmental models of disease transmission. *Mathematical Biosciences*, 180(1-2):29–48, November 2002. doi: 10.1016/s0025-5564(02)00108-6.

48. Amy Hurford, Daniel Cownden, and Troy Day. Next-generation tools for evolutionary invasion analyses. *Journal of The Royal Society Interface*, 7(45):561–571, April 2010. doi: 10.1098/rsif.2009.0448.
49. Mats Gyllenberg and Robert Service. Necessary and sufficient conditions for the existence of an optimisation principle in evolution. *Journal of Mathematical Biology*, 62(3):359–369, April 2010. ISSN 1432-1416. doi: 10.1007/s00285-010-0340-1.
50. Carl T. Bergstrom and Michael Lachmann. The red king effect: When the slowest runner wins the coevolutionary race. *Proceedings of the National Academy of Sciences*, 100(2): 593–598, January 2003. doi: 10.1073/pnas.0134966100.
51. Marcus R. Frean and Edward R. Abraham. Adaptation and enslavement in endosymbiont-host associations. *Phys. Rev. E*, 69:051913, 5 2004. doi: 10.1103/PhysRevE.69.051913.
52. Sylvie Estrela, J. Jeffrey Morris, and Benjamin Kerr. Private benefits and metabolic conflicts shape the emergence of microbial interdependencies. *Environmental Microbiology*, 18(5): 1415–1427, October 2015. ISSN 1462-2920. doi: 10.1111/1462-2920.13028.
53. Nancy A. Moran and Gordon M. Bennett. The tiniest tiny genomes. *Annual Review of Microbiology*, 68(1):195–215, September 2014. doi: 10.1146/annurev-micro-091213-112901.
54. John P. McCutcheon and Nancy A. Moran. Extreme genome reduction in symbiotic bacteria. *Nature Reviews Microbiology*, 10(1):13–26, November 2011. doi: 10.1038/nrmicro2670.
55. Rebecca A. Chong and Nancy A. Moran. Evolutionary loss and replacement of buchnera, the obligate endosymbiont of aphids. *The ISME Journal*, 12(3):898–908, January 2018. doi: 10.1038/s41396-017-0024-6.
56. N A Moran. Accelerated evolution and muller's rachet in endosymbiotic bacteria. *Proceedings of the National Academy of Sciences*, 93(7):2873–2878, April 1996. doi: 10.1073/pnas.93.7.2873.
57. John P. McCutcheon and Nancy A. Moran. Functional convergence in reduced genomes of bacterial symbionts spanning 200 my of evolution. *Genome Biology and Evolution*, 2: 708–718, January 2010. doi: 10.1093/gbe/evq055.
58. J. Jeffrey Morris, Richard E. Lenski, and Erik R. Zinser. The black queen hypothesis: Evolution of dependencies through adaptive gene loss. *mBio*, 3(2), May 2012. ISSN 2150-7511. doi: 10.1128/mbio.00036-12.
59. Filip Husnik, Naruo Nikoh, Ryuichi Koga, Laura Ross, Rebecca P. Duncan, Manabu Fujie, Makiko Tanaka, Nori Satoh, Doris Bachtrog, Alex C.C. Wilson, Carol D. von Dohlen, Takema Fukatsu, and John P. McCutcheon. Horizontal gene transfer from diverse bacteria to an insect genome enables a tripartite nested mealybug symbiosis. *Cell*, 153(7):1567–1578, June 2013. doi: 10.1016/j.cell.2013.05.040.
60. William H. Press and Freeman J. Dyson. Iterated prisoner's dilemma contains strategies that dominate any evolutionary opponent. *Proceedings of the National Academy of Sciences*, 109(26):10409–10413, 2012. doi: 10.1073/pnas.1206569109.
61. Benoit Daubech, Philippe Remigi, Ginaini Doin de Moura, Marta Marchetti, Cécile Pouzet, Marie-Christine Auriac, Chaitanya S Gokhale, Catherine Masson-Boivin, and Delphine Capela. Spatio-temporal control of mutualism in legumes helps spread symbiotic nitrogen fixation. *eLife*, 6, October 2017. ISSN 2050-084X. doi: 10.7554/elife.28683.
62. Susanne DiSalvo, Tamara S. Haselkorn, Usman Bashir, Daniela Jimenez, Debra A. Brock, David C. Queller, and Joan E. Strassmann. Burkholderia bacteria infectiously induce the proto-farming symbiosis of dictyostelium amoebae and food bacteria. *Proceedings of the National Academy of Sciences*, 112(36), August 2015. doi: 10.1073/pnas.1511878112.
63. Christian Kost, Kiran Raosaheb Patil, Jonathan Friedman, Sarahi L. Garcia, and Markus Ralser. Metabolic exchanges are ubiquitous in natural microbial communities. *Nature Microbiology*, 8(12):2244–2252, November 2023. ISSN 2058-5276. doi: 10.1038/s41564-023-01511-x.
64. Glen D'Souza and Christian Kost. Experimental evolution of metabolic dependency in bacteria. *PLOS Genetics*, 12(11):e1006364, November 2016. ISSN 1553-7404. doi: 10.1371/journal.pgen.1006364.
65. A. C. Darby and A. E. Douglas. Elucidation of the transmission patterns of an insect-borne bacterium. *Applied and Environmental Microbiology*, 69(8):4403–4407, August 2003. doi: 10.1128/aem.69.8.4403-4407.2003.
66. Takahiro Hosokawa, Yoshitomo Kikuchi, and Takema Fukatsu. How many symbionts are provided by mothers, acquired by offspring, and needed for successful vertical transmission in an obligate insect-bacterium mutualism? *Molecular Ecology*, 16(24):5316–5325, December 2007. doi: 10.1111/j.1365-294x.2007.03592.x.
67. P. Buchner. *Endosymbiosis of Animals with Plant Microorganisms*. Wiley, 1965. ISBN 9780470115176.
68. E Akman Gündüz and A.E Douglas. Symbiotic bacteria enable insect to use a nutritionally inadequate diet. *Proceedings of the Royal Society B: Biological Sciences*, 276(1658):987–991, December 2008. doi: 10.1098/rspb.2008.1476.
69. Kevin J. Vogel and Nancy A. Moran. Sources of variation in dietary requirements in an obligate nutritional symbiosis. *Proceedings of the Royal Society B: Biological Sciences*, 278 (1702):115–121, July 2010. doi: 10.1098/rspb.2010.1304.
70. Horst Felbeck and Janka Jarchow. Carbon release from purified chemoautotrophic bacterial symbionts of the hydrothermal vent tubeworm riftia pachyptila. *Physiological Zoology*, 71 (3):294–302, May 1998. doi: 10.1086/515931.
71. Claire L. Scarborough, Julia Ferrari, and H. C. J. Godfray. Aphid protected from pathogen by endosymbiont. *Science*, 310(5755):1781–1781, December 2005. doi: 10.1126/science.1120180.
72. Lukas Gehrer and Christoph Vorburger. Parasitoids as vectors of facultative bacterial endosymbionts in aphids. *Biology Letters*, 8(4):613–615, March 2012. doi: 10.1098/rsbl.2012.0144.
73. E. Toby Kiers, Robert A. Rousseau, Stuart A. West, and R. Ford Denison. Host sanctions and the legume–rhizobium mutualism. *Nature*, 425(6953):78–81, September 2003. doi: 10.1038/nature01931.
74. R. Ford Denison and E. Toby Kiers. Life histories of symbiotic rhizobia and mycorrhizal fungi. *Current Biology*, 21(18):R775–R785, September 2011. doi: 10.1016/j.cub.2011.06.018.
75. Harald Ronald Gruber-Vodicka, Ulrich Dirks, Nikolaus Leisch, Christian Baranyi, Kilian Stoecker, Silvia Bulgheresi, Niels Robert Heindl, Matthias Horn, Christian Lott, Alexander Loy, Michael Wagner, and Jörg Ott. Paracatenula, an ancient symbiosis between thiotrophic alphaproteobacteria and catenulid flatworms. *Proceedings of the National Academy of Sciences*, 108(29):12078–12083, June 2011. doi: 10.1073/pnas.1105347108.
76. John P. McCutcheon, Bradon R. McDonald, and Nancy A. Moran. Convergent evolution of metabolic roles in bacterial co-symbionts of insects. *Proceedings of the National Academy of Sciences*, 106(36):15394–15399, September 2009. doi: 10.1073/pnas.0906424106.
77. GS Losey, A Grutter, G Rosenquist, JL Mahon, and J Zamzow. Cleaning symbiosis: a review. In *Behaviour and Conservation of Littoral Fishes*. ISPA, 1999.
78. Leah Edelstein-Keshet. *Mathematical Models in Biology*. Society for Industrial and Applied Mathematics, January 2005. doi: 10.1137/1.9780898719147.

Supplementary Note S1: Mathematical details of the model

A. Traits and their relation to ecological parameters. Here we make explicit the interpretations of the traits Ω_i and α_i. Recall that the obligacies Ω_i formalise a tradeoff between individual and collective reproduction. Further, the obligacy of an independent host does not affect the growth rate of the independent symbiont; the two traits only interact through their impact on the growth rate of the collective. Hence, if the growth rates of the three types are f_H, f_S, f_C, then the corresponding constraints are

$$\frac{\partial f_i}{\partial \Omega_i} \leq 0; \qquad \frac{\partial f_C}{\partial \Omega_i} \geq 0; \qquad \frac{\partial f_i}{\partial \Omega_j} = 0, \qquad i \neq j \in \{H,S\}. \tag{S1}$$

Therefore the intrinsic growth rate f_i of the population of species i is a function only of its own obligacy Ω_i. Lastly, neither the host nor the symbiont can reproduce independently when its obligacy is 1, so $f_i(\Omega_i = 1) = 0, i \in \{H,S\}$, and the collective cannot reproduce as a unit whenever any one of the host or symbiont are at zero obligacy: $f_C(\Omega_H, 0) = f_C(0, \Omega_S) = 0 \; \forall \; \Omega_H, \Omega_S \in [0,1]$. We assume that $f_i \geq 0 \; \forall \; i \in \{H,S,C\}$.
The adhesions α_i formalise a tradeoff between synchronised and asynchronised reproduction. Therefore a higher adhesion increases the rate of association, increases the rate of collective reproduction, and decreases the rate of dissociation. If a is the rate of association and d is the rate of dissociation, we impose the constraints

$$\frac{\partial f_C}{\partial \alpha_i} \geq 0; \qquad \frac{\partial a}{\partial \alpha_i} \geq 0; \qquad \frac{\partial d}{\partial \alpha_i} \leq 0, \qquad i \in \{H,S\}. \tag{S2}$$

As rates, $a, d \geq 0$ at all trait values, and we assume that at $\alpha_H = \alpha_S = 0$, a is minimum and d is maximum; conversely at $\alpha_H = \alpha_S = 1$, a is maximum and d is minimum.
An example of equations that satisfy all these constraints is the following, and is the one (or variations thereof) we use across the main text:

$$\begin{aligned} f_H(\Omega_H, \alpha_H, \Omega_S, \alpha_S) &= r_H(1-\Omega_H), \\ f_S(\Omega_H, \alpha_H, \Omega_S, \alpha_S) &= r_S(1-\Omega_S), \\ f_C(\Omega_H, \alpha_H, \Omega_S, \alpha_S) &= r_C \Omega_H \Omega_S \alpha_H \alpha_S, \\ d(\Omega_H, \alpha_H, \Omega_S, \alpha_S) &= d_0(1-\alpha_H \alpha_S), \\ a(\Omega_H, \alpha_H, \Omega_S, \alpha_S) &= a \in \mathbb{R}_{\geq 0}. \end{aligned} \tag{S3}$$

When the adhesions are held constant, this can be described by

$$\begin{aligned} f_H(\Omega_H, \alpha_H, \Omega_S, \alpha_S) &= r_H(1-\Omega_H), \\ f_S(\Omega_H, \alpha_H, \Omega_S, \alpha_S) &= r_S(1-\Omega_S), \\ f_C(\Omega_H, \alpha_H, \Omega_S, \alpha_S) &= r_C \Omega_H \Omega_S. \end{aligned} \tag{S4}$$

and when we assume obligacies to be constant, we model the ecological consequences of a different adhesion via:

$$\begin{aligned} f_C(\Omega_H, \alpha_H, \Omega_S, \alpha_S) &= r_C \alpha_H \alpha_S \\ d(\Omega_H, \alpha_H, \Omega_S, \alpha_S) &= d_0(1-\alpha_H \alpha_S) \\ a(\Omega_H, \alpha_H, \Omega_S, \alpha_S) &= a_0 \in \mathbb{R}_{\geq 0} \end{aligned} \tag{S5}$$

B. Correspondence to a symmetric mutualism model. It is useful to establish the ecological context of our model and understand exactly how the presence of a collective affects the independent types. One can do this by comparing an extreme version (colloquially, "take a limit") of our exponential model (Eq. system 8 in the main text) to more familiar models in the following way. Recall the population dynamics in the exponential model:

$$\begin{aligned} \dot{x}_H &= f_H x_H \left(1 - \frac{x_H}{K_H}\right) - a x_H x_S + d x_C, \\ \dot{x}_S &= f_S x_S \left(1 - \frac{x_S}{K_S}\right) - a x_H x_S + d x_C, \\ \dot{x}_C &= f_C x_C + a x_H x_S - d x_C. \end{aligned} \tag{S6}$$

In all of our analyses, we are only interested in long-term symbioses like the nutrient-exchange symbioses in anaerobic ciliates (21), and not symbioses where the interaction is short-lived, like the parasite-cleaning mutualisms (77). If the interaction

between the participants is ephemeral, the collective does not have as much of an independent existence. In the limiting case of instantaneous interaction, we can set $\dot{x}_C = 0$. This has the effect of reducing the system of population dynamics equations Eq. (S6) to

$$\dot{x}_H = f_H x_H (1 - \frac{x_H}{K_H}) + \left(\frac{ad}{d - f_C} - a\right) x_H x_S \,,$$
$$\dot{x}_S = f_S x_S (1 - \frac{x_S}{K_S}) \;\; + \left(\frac{ad}{d - f_C} - a\right) x_H x_S \,.$$

It is easily read off from this set of equations that there is now a constant k preceding the cross-term $x_H x_S$ in both equations, with

$$k = a\left(\frac{d}{d - f_C} - 1\right).$$

Since $f_C > 0$ by assumption, $d > d - f_C$ and therefore $k > 0$ as long as $d > f_C$. This last condition implies that the interaction is beneficial as long as $d > f_C$ and becomes detrimental to both species when the collective growth rate f_C is "too high" - larger than d. Reinterpreting this cross-term $k x_H x_S$ as arising from a Lotka-Volterra-type interaction, one arrives at the conclusion that the formation of a collective, in this "limit", is equivalent to a symmetric mutualism as long as the dissociation is strong enough. If it is too weak, it goes from being a mutualism to being an interaction that is negatively affecting the growth of both parties. That it is symmetric in either case reflects the fact that with every collective reproduction event, there is exactly one new host and one new symbiont. This shows that collective reproduction can indeed be thought of as aligning reproductive interests of the host and symbiont. Like in a mutualism, the investment of one of the types (H or S) in collective reproduction therefore helps the other.

Supplementary Note S2: Existence, dynamical stability, and variation of equilibrium population sizes

A. Logistic model. The following figures show the variation of equilibrium population sizes (x_H^*, x_S^*, x_C^*) as a function of the obligacies (Ω_H, Ω_S) (Fig. S1) and the adhesions (α_H, α_S) (Fig. S2). All figures are in the form of heatmaps, and are obtained by Forward Euler-numerical integration of the population dynamical equations

$$\begin{aligned}
\dot{x}_H &= f_H x_H \left(1 - \frac{x_H}{K_H}\right) - a x_H x_S + d x_C, \\
\dot{x}_S &= f_S x_S \left(1 - \frac{x_S}{K_S}\right) - a x_H x_S + d x_C, \\
\dot{x}_C &= f_C x_C \left(1 - \frac{x_C}{K_C}\right) + a x_H x_S - d x_C.
\end{aligned} \tag{S7}$$

The above system is Eq. 1 in the main text. It is useful to note first of all that the routine found non-negative fixed points, and so one can say that biologically meaningful equilibria exist over a large range of parameters (over all values of traits, and over different values of r_C, K_C). Further, since the below equilibria were found by numerical integration, they are all necessarily stable (in the sense of a fixed point of a dynamical system). Third, the gradual change of the colours in the heatmap as the traits change suggests that it is in reality a single fixed point that changes location based on the trait values.

B. Exponential model. The exponential model of population dynamics (Eq. (S6)) has four fixed points for the population densities, three of which are trivial. These trivial fixed points are located on the boundary at $(0,0,0), (K_H,0,0)$ and $(0,K_S,0)$. The internal fixed point is given by

$$\begin{aligned}
x_H^* &= \frac{K_H f_S (f_C - d)(a K_S f_C + (d - f_C) f_H)}{a^2 K_H K_S f_C^2 - f_H f_S (d - f_C)^2}, \\
x_S^* &= \frac{K_S f_H (f_C - d)(a K_H f_C + (d - f_C) f_S)}{a^2 K_H K_S f_C^2 - f_H f_S (d - f_C)^2}, \\
x_C^* &= \frac{a f_S f_H K_S K_H (d - f_C)(a K_S f_C + (d - f_C) f_H)(a K_H f_C + (d - f_C) f_S)}{[a^2 K_H K_S f_C^2 - f_H f_S (d - f_C)^2]^2}.
\end{aligned} \tag{S8}$$

The interal fixed point (x_H^*, x_S^*, x_C^*) is internal, and feasible, i.e., all equilibrium densities are non-negative when

$$d > f_C \left(1 + a\sqrt{\frac{K_H K_S}{f_H f_S}}\right). \tag{S9}$$

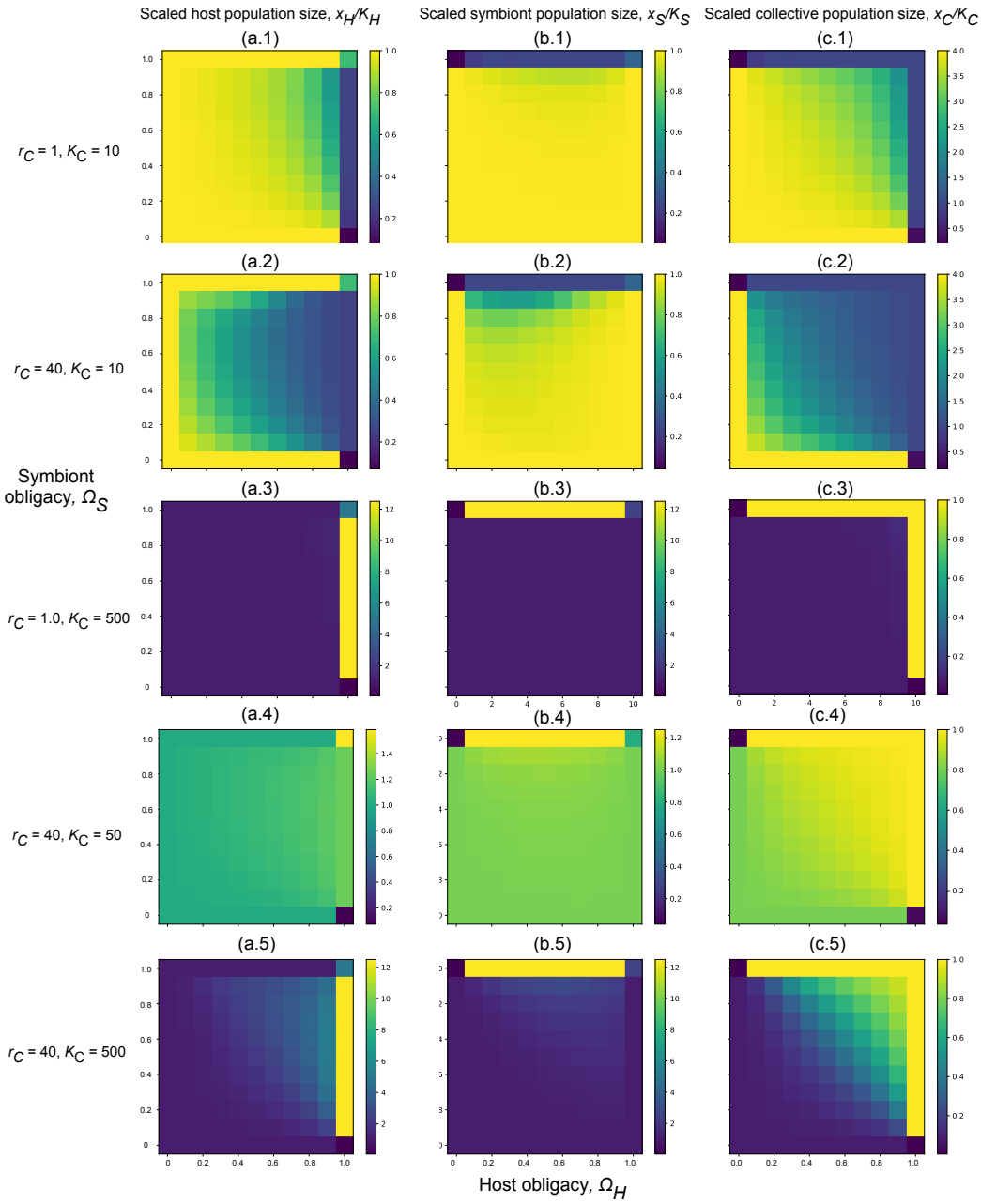

Fig. S1. These panels contain heatmaps of the scaled equilibrium population sizes x_i^*/K_i as functions of the obligacies Ω_i, for five combinations of r_C and K_C. The first column (panels a.1 to a.5) corresponds to host population size, panels b.1 to b.5 to symbiont population size, and the last column to collective population size. The data for a given cell in a given heatmap is obtained by running a numerical integration routine (forward Euler) of Eq. (S7) starting from the initial conditions $(x_H, x_S, x_C)(0) = (10, 10, 0)$. The mapping from the traits to parameters is given by $f_H = r_H(1-\Omega_H), f_S = r_S(1-\Omega_S), f_C = r_C\Omega_H\Omega_S$. **Parameter values.** $r_H = 8, r_S = 20, K_H = 100, K_S = 200, a = 0.1, d = 50$.

To establish the condition for feasibility, first notice that any fixed point must satisfy

$$x_C^* = \frac{a}{d - f_C} x_H^* x_S^*, \tag{S10}$$

which arises from setting the dynamical equation for x_C to zero. First, notice that neither x_H^* nor x_S^* can be negative since we are searching for feasible equilibria. Therefore, we require $d > f_C$ since otherwise x_C^* cannot be positive. The expressions for the host and symbiont population size have a similar form - they are, after all, symmetric in their attributes. Notice that the numerators of x_H^* and x_S^* are negative whenever $d > f_C$. Therefore, the expressions x_H^*, x_S^* on the whole are positive whenever the denominator is also (strictly) negative. Then notice that they have the same denominator. The negativity of the denominator, upon rearranging to solve for d, exactly gives rise to the feasibility bound. Further, we determined computationally that this

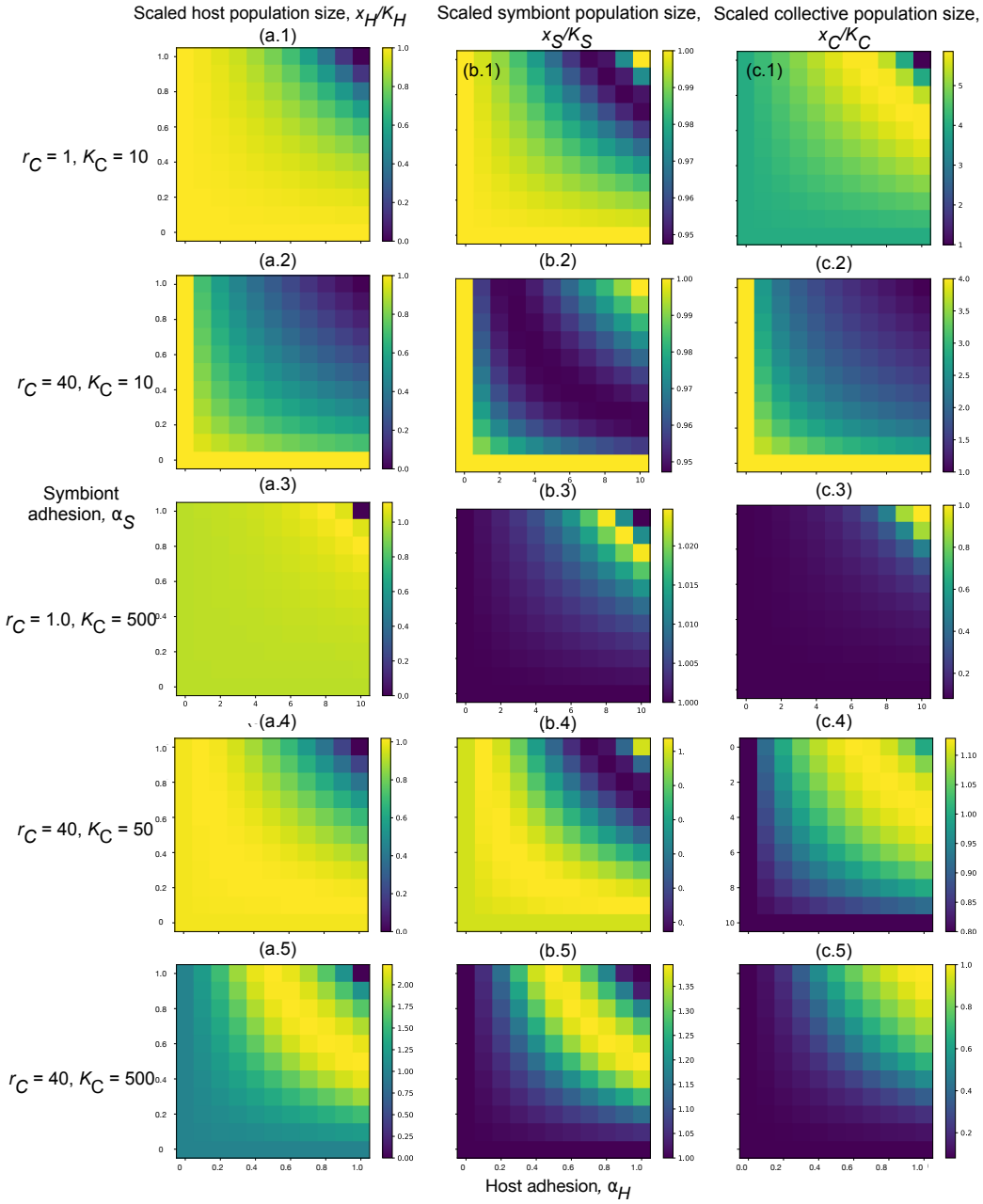

Fig. S2. These panels contain heatmaps of the scaled equilibrium population sizes x_i^*/K_C as functions of the adhesions α_i, for five combinations of r_C and K_C. The first column (panels a.1 to a.4) corresponds to host population size, panels b.1 to b.4 to symbiont population size, and the last column to collective population size. The data for a given cell in a given heatmap is obtained by running a numerical integration routine (forward Euler) of Eq. (S7) starting from the initial conditions $(x_H, x_S, x_C)(0) = (10, 10, 0)$. The mapping from the traits to parameters is given by $d = d_0(1-\alpha_H\alpha_S), f_C = r_C\alpha_H\alpha_S, a = a_0 \in \mathbb{R}\ \forall \alpha_i$. **Other parameter values.** $d_0 = 50, a = 0.1, f_H = 8, f_S = 20, K_H = 100, K_S = 200$.

inequality guarantees linear stability for a large range of parameters (Fig. S3). Note that this lower bound on d is strictly larger than f_C.

The next step is to find conditions for the stability of the equilibrium. The Jacobian of this system is given by

$$J = \begin{pmatrix} f_H(1-\frac{2x_H}{K_H}) - ax_S & -ax_H & d \\ -ax_S & f_S(1-\frac{2x_S}{K_S}) - ax_H & d \\ ax_S & ax_H & f_{HS} - d \end{pmatrix}. \tag{S11}$$

In the case of the trivial fixed point $(0,0,0)$, the Jacobian above becomes upper triangular. The eigenvalues of a diagonal matrix are exactly the elements on its diagonal, and two of these elements are f_H and f_S. We assume that these quantities are always

positive in the entirety of this work, so this fixed point is never stable. It is not as easy for the other fixed points: the roots computed directly from the general characteristic equation are required and difficult to analyse, and we therefore resort to the Routh-Hurwitz criteria (78). This is a set of criteria on the coefficients in the characteristic equation of J. Specifically, let the characteristic equation be given by

$$\lambda^3 + a_1\lambda^2 + a_2\lambda + a_3 = 0\,.$$

These numbers a_i are computable directly from J, and some of them are commonly known. For example, a_1 above is the negative of the trace of J, and a_3 is the negative of its determinant. The Routh-Hurwitz criteria state that all eigenvalues of J, i.e., all roots of the above polynomial, have a negative real part if and only if

$$\begin{aligned} a_1 &> 0\,, \\ a_3 &> 0\,, \\ a_1 a_2 &> a_3\,. \end{aligned} \tag{S12}$$

We shall not give the expressions for these coefficients a_i here, they can be found in the associated Mathematica notebook ('./Analytics/obligacy-evolution.nb').

For the two one-species equilibria $(K_H, 0, 0)$ and $(0, K_S, 0)$, the criteria can be verified easily: as long as the interior fixed point is feasible, these equilibria are unstable - one of the criteria above Eq. (S12) fails since $d > f_C$. In particular, the feasibility bound being satisfied implies that $a_3 < 0$ in these two cases. Further, there is a parameter range where none of the fixed points are stable: this is exactly when

$$f_C < d < f_C\left(1 + a\sqrt{\frac{K_H K_S}{f_H f_S}}\right)\,.$$

This is when the feasibility bound is violated (which is the right side of the above chain of inequalities), but not as strongly as to make $f_C > d$ (left side of the chain). Therefore, the internal fixed point is rendered unstable, as well as all other fixed points: the only outcome for the abundances can be to escape to infinity.

For the internal equilibrium, the picture is much more involved. We cannot say much from the coefficients a_i themselves, but it can be shown that the subcriterion $a_3 > 0$ exactly corresponds, upon some rearrangement, to the inequality that we have termed the feasibility bound. This proves that feasibility is necessary for stability.

Further analytics is difficult, and we therefore resort to numerically computing the maximum real part of the eigenvalues of J across a biologically reasonable range of parameter space. The results of this exercise are shown in Figure S3. This shows that the internal fixed point of the exponential model is, in fact, stable in the region of parameter space that we are interested in, and therefore, we proceed with further analysis.

Supplementary Note S3: Independent trait evolution under the logistic model

A. Adhesion evolution when host and symbiont are identical. Figure S4 demonstrates that the difference in host and symbiont population parameters induces the difference in their respective adhesion values' evolutionary outcomes. The biologically realistic case is for r_S and K_S to be higher than the host counterparts, and this leads to the long run outcome $\alpha_H < 1, \alpha_S = 1$. It is trivial to observe that this outcome is flipped if the host now has the higher r, K – host and symbiont are just exogenously imposed labels, and can be flipped so that the old symbiont is called the "host". In this figure, we show that if $r_H = r_S, K_H = K_S$ then there is no asymmetry in the trajectories – both host and symbiont adhesions stop short of (1,1) because it is not advantageous to go downhill from the local maximum in x_i^* (as explained in the main text, using the support of Figure S2). Due to the stochastic nature of these simulations, some trajectories can escape to either side of the boundary; importantly, note that this happens in both host and symbiont trajectories.

B. A sufficient condition for evolution to high Ω_i or α_i. We claim that the following is a sufficient condition for the evolution of high obligacies or high adhesions:

$$K_C > \frac{aK_H K_S}{d}\,.$$

In particular, the right-hand side is the equilibrium population size of the collective that can be maintained by pure association and dissociation, i.e., how large the collective population is when $f_C = 0$, no synchronised reproduction.

In Figure 4 of the main text, the parameter values are: $a = 0.1, d = 50, r_H = 8, r_S = 20, r_C = 40, K_H = 100, K_S = 200$. Therefore the value of $\frac{aK_H K_S}{d}$ is 40. Our low value of K_C is 10, and the high value is 500, therefore satisfying the claim so far.

We tested the claim further by changing the value of a in two ways: first to decrease the value of a when $K_C = 10$ – this would push down the threshold $\frac{aK_H K_S}{d}$ and make K_C high enough under our claim. The second test is to increase the value of a when $K_C = 500$, in an attempt to make $K_C = 500$ lower than the threshold. Both tests lead to results that support this criterion:

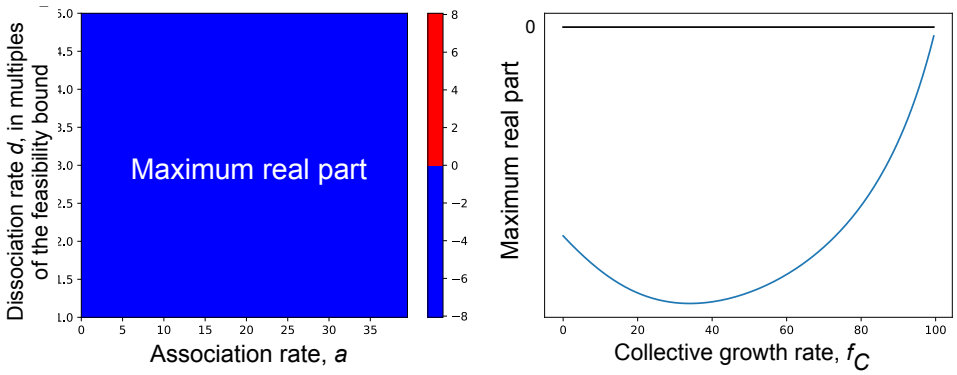

Fig. S3. The internal fixed point of the exponential model is stable. Here we perform a numerical evaluation of the stability condition of the internal fixed point of the exponential model. In particular, we find and plot in two cases, the maximum real part of the eigenvalues of J, the Jacobian of the flow Eq. (S6). **Common parameter values for both panels.** $K_H = 100, K_S = 200, f_H = 8, f_S = 20$. **(a)** Red if unstable, blue if stable. Since we can already show that the feasibility bound is necessary for stability (see §B, we wish to only check stability when the feasibility bound is already satisfied. This panel is therefore a little unorthodox – the x-axis is the usual, but the y-axis is in multiples above the feasibility bound for the respective x value. Let $d_f(a) = f_C(1 + a\frac{K_H K_S}{f_H f_S})$ be the equalising value of d at the feasibility bound when all other parameters are kept fixed. Then in the heatmap, for a given value of the horizontal variable a, the vertical strip at this horizontal position ranges from $[d_f(a), 5 \times d_f(a)]$. This panel therefore shows that the fixed point is stable for a large range of d values once the feasibility bound is crossed. **Parameter values.** $f_C = 10, a \in [0, 40], d \in [d_f(a), 5 \times d_f(a)]$ **(b)** This shows that the fixed point is stable across a range of f_C values. **Parameter values.** $a = 0.1, f_C \in [0, 5f_S = 100], d = a + f_{C,\text{max}}(1 + a\sqrt{\frac{C_H C_S}{f_H f_S}})$ to maintain feasibility.

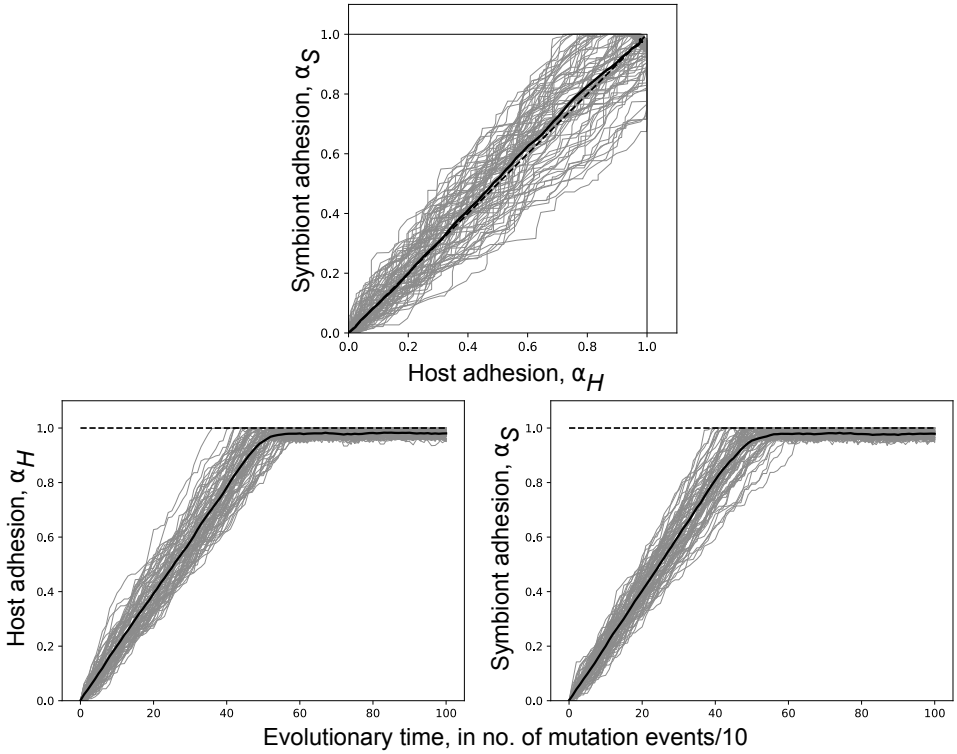

Fig. S4. Adhesion evolution when host and symbiont are identical. Parameter values. $a = 0.1, d = 50, K_H = K_S = 100, K_C = 500, r_C = 10, r_H = r_S = 8$.

when $a = 0.01$, obligacies evolve to high values even when $K_C = 10$ (Fig. S5); when $a = 5$, obligacies remain at (0,0) even when $K_C = 500$.

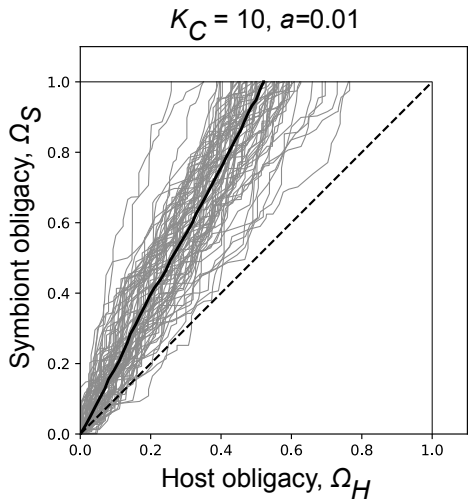

Fig. S5. Parameter values. $d = 50, r_C = 40, K_H = 100, K_S = 200, 500, r_H = 8, r_S = 20.$

However, due to a lack of analytical expressions, it is difficult to prove if this is also a necessary condition.

C. Can (α_H, α_S) ever get to (1,1)?. Adhesion values can indeed reach (1,1) if K_C is high enough (see Figure S6). It can, of course, be argued that there is a point attractor at (1,1) that is only reached after infinite time and when $K_C \to \infty$, and that we only see it as (1,1) in these data due to the inherently discretised nature of simulations. However, this "one is only the supremum" interpretation is also good enough: the bottom line is that there is no upper bound on α_H that restricts it always to values less than 1.

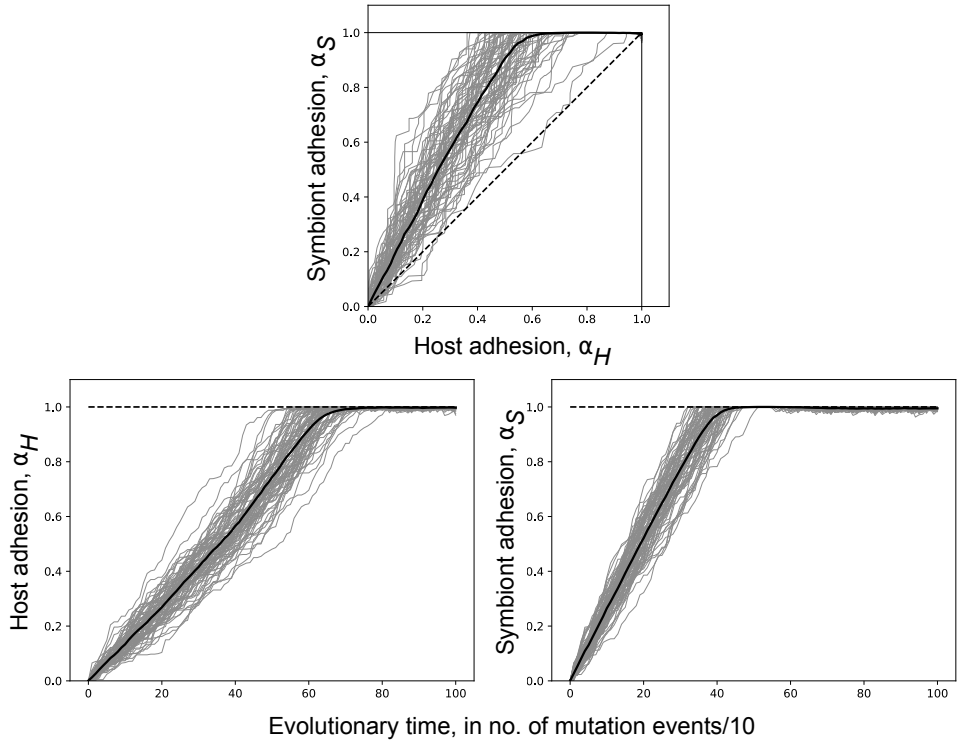

Fig. S6. Parameter values. $a = 0.1, d = 50, K_H = K_S = 100, K_C = 10000, r_C = 40, f_H = 8, f_S = 20.$

D. The effect of within-collective reproduction and mortality rates, additional figures. We reproduce the logistic model with within-collective birth and death rates (Eq. 6 in the main text) here for convenience:

$$\begin{aligned}
\dot{x}_H &= f_H x_H \left(1 - \frac{x_H}{K_H}\right) - a x_H x_S + d x_C + (d_S + b_H) x_C, \\
\dot{x}_S &= f_S x_S \left(1 - \frac{x_S}{K_S}\right) - a x_H x_S + d x_C + (d_H + b_S) x_C, \\
\dot{x}_C &= f_C x_C \left(1 - \frac{x_C}{K_C}\right) + a x_H x_S - d x_C - (d_S + d_H) x_C.
\end{aligned} \tag{S13}$$

The effect of different values of d_i on the obligacies is presented in Fig. Eq. (S7), and the effect of different b_i values on obligacies is in Fig. Eq. (S9). The effect of different b_i and d_i on adhesions is presented in Fig. Eq. (S8).

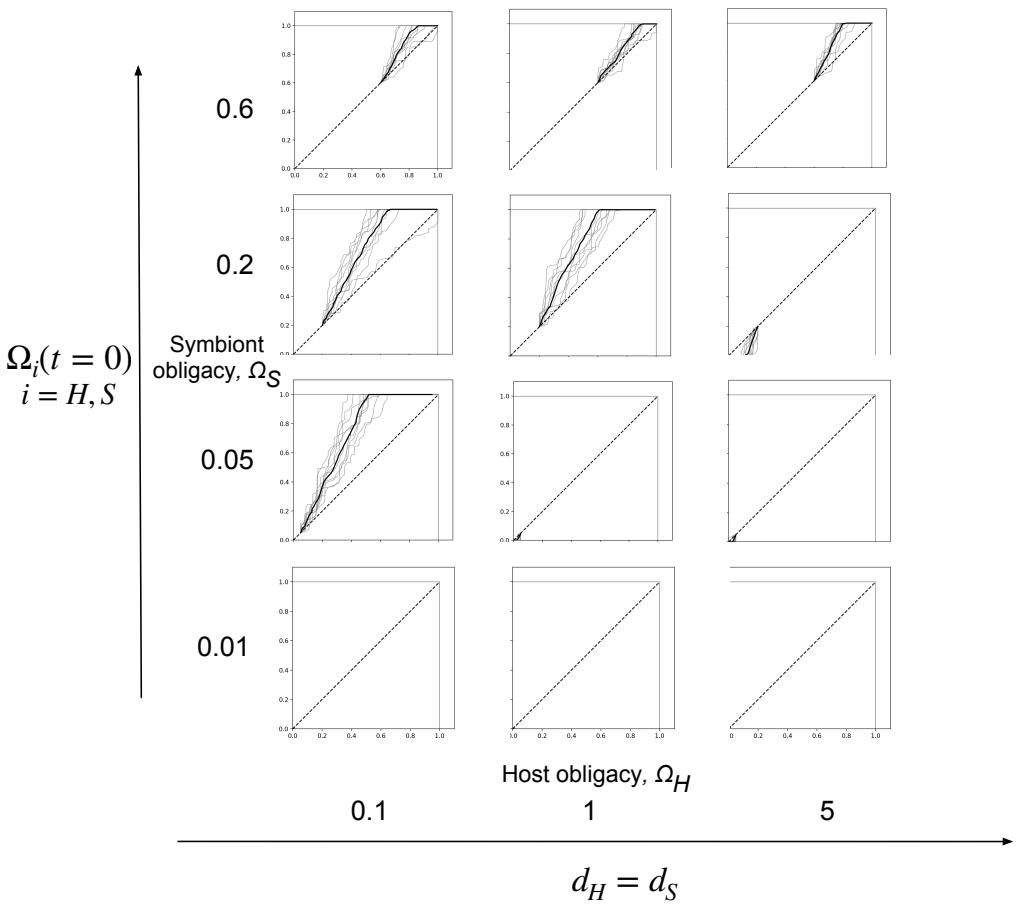

Fig. S7. Adding a death term to obligacy evolution. **Parameters:** same as main text, $r_H = 8, r_S = 20, r_C = 10, K_H = 100, K_S = 200, K_C = 250, a = 0.1, d = 50, d_H = d_S \in \{0.1, 1, 5\}$

Supplementary Note S4: Deriving and using an invasion criterion

The population dynamical equations under the logistic model are given in the main text as Eq. system 1 and as Eq. S7 in this document.

To compute the invasion fitness of an arbitrary mutant, we suppose that there is a resident population with host and symbiont traits (Ω_H, α_H) and (Ω_S, α_S), respectively. After a sufficiently long time, a mutant arises when the resident population is at equilibrium, say with population sizes (x_H^*, x_S^*, x_C^*). Due to the separation between ecological and evolutionary timescales, there can only be one mutant at a time, without loss of generality, say a host mutant. This mutant has trait value $(\tilde{\Omega}_H, \tilde{\alpha}_H)$ different from the resident, giving rise to different values of the parameters $\tilde{f}_H, \tilde{f}_C, \tilde{a}, \tilde{d}$ for the mutant host. The invasion condition is formalised as follows: we augment the model Eq. (S7) with additional equations tracking each type that arises due to the introduction of a mutant. Here, this always amounts to two more – the mutant host y_H itself and the mutant host-resident

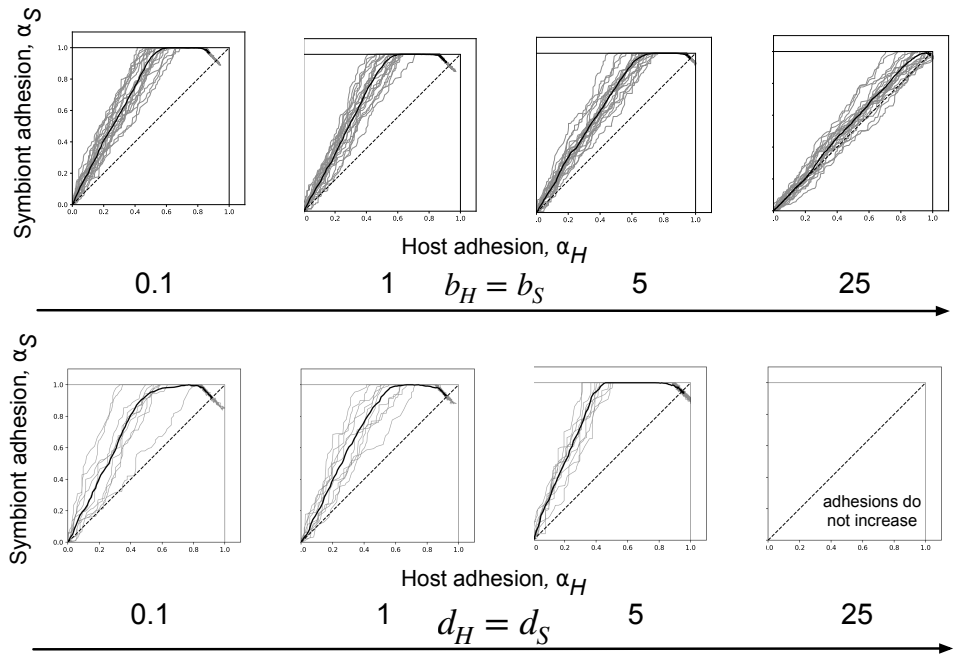

Fig. S8. Adhesion evolution under within-collective birth and death terms. **Parameters:** same as main text, $f_H = 8, f_S = 20, r_C = 10, K_H = 100, K_S = 200, K_C = 250, a = 0.1, d_0 = 50$. Top row: $d_H = d_S \in \{0.1, 1, 5, 25\}$, bottom row: $d_H = d_S \in \{0.1, 1, 5, 25\}$

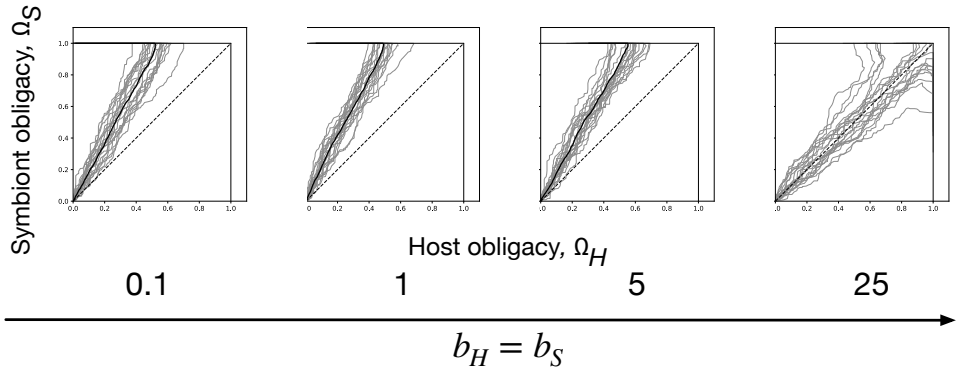

Fig. S9. Obligacy evolution under within-collective birth term. **Parameters:** same as main text, $r_H = 8, r_S = 20, r_C = 10, K_H = 100, K_S = 200, K_C = 250, a = 0.1, d = 50, b_H = b_S \in \{0.1, 1, 5, 25\}$

symbiont collective y_C. The augmented model takes the form

$$
\begin{aligned}
\dot{x}_H &= f_H x_H \left(1 - \frac{x_H + y_H}{K_H}\right) - a x_H x_S + d x_C \,, \\
\dot{x}_S &= f_S x_S \left(1 - \frac{x_S}{K_S}\right) - a(x_H + y_H) x_S + d(x_C + y_C) \,, \\
\dot{x}_C &= f_C x_C \left(1 - \frac{x_C + y_C}{K_C}\right) + a x_H x_S - d x_C \,, \\
\dot{y}_H &= \tilde{f}_H x_H \left(1 - \frac{x_H + y_H}{K_H}\right) - \tilde{a} y_H x_S + \tilde{d} y_C \,, \\
\dot{y}_C &= \tilde{f}_C y_C \left(1 - \frac{x_C + y_C}{K_C}\right) + \tilde{a} y_H x_S - \tilde{d} y_C \,.
\end{aligned}
\tag{S14}
$$

The invasion fitness is interpreted to be the growth rate of a rare mutant in a resident population that is at stable equilibrium

(37). For a mutant host, this Jacobian (when the mutant is rare i.e., $y_H = y_C = 0$) takes the form

$$J = \begin{pmatrix} f_H(1-\frac{2x_H}{K_H}) - ax_S & -ax_H & d & -\frac{f_H x_H}{K_H} & 0 \\ -ax_S & f_S(1-\frac{2x_S}{K_S}) - ax_H & d & -\tilde{a}x_S & \tilde{d} \\ ax_S & ax_H & f_C - d & 0 & 0 \\ 0 & 0 & 0 & \tilde{f}_H\left(1-\frac{x_H}{K_H}\right) - ax_S & \tilde{d} \\ 0 & 0 & 0 & \tilde{a}x_S & \tilde{f}_C\left(1-\frac{x_C}{K_C}\right) - \tilde{d} \end{pmatrix}. \tag{S15}$$

Due to the block-upper-triangular form of J, its eigenvalues are given entirely by the eigenvalues of only its diagonal blocks. We know the top-left 3×3 block has all eigenvalues with negative real part since we began with a stable population dynamical equilibrium. Therefore, we need only check the dominant eigenvalue of the submatrix corresponding to the mutant, i.e., the bottom right 2×2 block. The invasion fitness is thus defined as the dominant eigenvalue of the "sub-Jacobian" corresponding to the mutant equations, evaluated at $(x_H^*, x_S^*, x_C^*, y_H = 0, y_C = 0)$:

$$\begin{bmatrix} \tilde{f}_H x_H^*\left(1-\frac{x_H^*}{K_H}\right) - \tilde{a}x_S^* & \tilde{d} \\ \tilde{a}x_S^* & \tilde{f}_C\left(1-\frac{x_C^*}{K_C}\right) - \tilde{d} \end{bmatrix}.$$

If it is positive, the equilibrium is destabilised in the presence of the mutant and the mutant can invade; if it is negative, the mutant goes to extinction (38, 46). This quantity is unwieldy and not amenable to mathematical analysis in our case, so we turn to other methods to quantify (in)stability of the resident population in response to mutants.

In particular, we use the next-generation theorem, which gives, under some conditions, an alternate characterisation of the standard stability condition of all eigenvalues having negative real parts (47, 48). Concretely, suppose we have a linear system of ODEs given by

$$\dot{\mathbf{x}} = A\mathbf{x},$$

and the matrix A can be decomposed in terms of two matrices F and V as $A = F - V$, with some conditions on F and V. Now define $s(M)$ to be the maximum real part of all the eigenvalues of a matrix M, and $\rho(M)$ to be the maximum modulus of all the eigenvalues. The next-generation theorem (47) states that $s(A) = s(F-V)$ has the same sign as $\rho(F.V^{-1}) - 1$. The quantity $\rho(F.V^{-1})$ is exactly the R_0 value usually associated with the spread of virulent pathogens, and describes the average number of offspring one mutant individual sires. If it is larger than 1, then the mutant spreads. Therefore, if we can find a satisfactory decomposition $J = F - V$ of J in Equation Eq. (S15), the fixed point in question is stable if and only if $\rho(F.V^{-1}) - 1 > 0$. This alternative method is useful because the latter quantity is sometimes more analytically tractable and interpretable than $s(J)$.

A. A useful but incomplete invasion criterion for the logistic model. For the logistic model, one can use the decomposition given by

$$F = \begin{bmatrix} \tilde{f}_H & \tilde{d} \\ 0 & 0 \end{bmatrix} \tag{S16}$$

$$V = \begin{bmatrix} \tilde{a}x_S + \frac{\tilde{f}_H(x_H)}{K_H} & 0 \\ -\tilde{a}x_S & \tilde{d} - \tilde{f}_C + \frac{\tilde{f}_C(x_C)}{K_C} \end{bmatrix} \tag{S17}$$

which satisfies all the requirements – all entries of F are positive, all eigenvalues of $-V$ are negative (we assume that $\tilde{d} - \tilde{f}_C + \frac{\tilde{f}_C(x_C)}{K_C}$ stays positive), and all elements of V^{-1} are negative.

This leads to the invasion criterion

$$\frac{\tilde{f}_H + \frac{\tilde{d}\tilde{a}x_S^*}{(\tilde{d}-\tilde{f}_C)+\tilde{f}_C\frac{x_C^*}{K_C}}}{\tilde{f}_H\frac{x_H^*}{K_H} + ax_S^*} > 1 \tag{S18}$$

for a host mutant with traits $(\tilde{\Omega}_H, \tilde{\alpha}_H)$ to invade a resident population composed of hosts having traits (Ω_H, α_H) and symbionts (Ω_S, α_S). Tilde-d quantities are functions of the tilde-d traits, and we assume a is independent of the trait values. Of course, a similar (but mirrored in H and S) expression exists for the invasion of a symbiont mutant. Although we know that the population sizes are themselves positive, it is difficult to solve exactly for when this quantity as a whole is positive because we do not possess expressions for x_i^* in terms of the other variables and parameters. However, we can use this to understand edge cases when we can indeed find the equilibrium population sizes analytically.

For example, one useful case is to consider $\Omega_S = 1, \Omega_H < 1$. Then $r_S = 0$, and the symbiont is sustained only by association and dissociation. This implies that at equilibrium, $x_S^* = \frac{a x_H^*}{d x_C^*}$. Further, since the association and dissociation must balance (see $\dot{x}_S$ in Eq. (S7)), it follows that the host and collective populations must (each) be at either zero or their respective carrying capacities. Using this in R_0 shows that it is exactly equal to 1, meaning that from here on, the value of Ω_H is not under selection.

B. An exact invasion criterion for the exponential model. For the exponential model, we can use a similar decomposition

$$F = \begin{bmatrix} \tilde{f}_H & \tilde{d} \\ 0 & 0 \end{bmatrix} \tag{S19}$$

$$V = \begin{bmatrix} \tilde{a} x_S + \frac{\tilde{f}_H(x_H)}{K_H} & 0 \\ -\tilde{a} x_S & \tilde{d} - \tilde{f}_C \end{bmatrix} \tag{S20}$$

$$V^{-1} = \begin{bmatrix} \frac{K_H}{a K_H \tilde{x}_S + \tilde{f}_H(x_H)} & 0 \\ \frac{a x_S K_H}{(\tilde{d} - \tilde{f}_C)(a K_H \tilde{f}_S + \tilde{f}_H(x_H))} & \frac{1}{\tilde{d} - \tilde{f}_C} \end{bmatrix} \tag{S21}$$

We also require that $\tilde{f}_C < \tilde{d}$ in the mutant host case, just as has been shown to be necessary for the existence of a feasible resident equilibrium. We now restrict ourselves to finding the condition under which $\rho(F.V^{-1}) - 1 > 0$. This leads directly to the invasion criterion

$$\frac{\widetilde{f}_H}{\widetilde{a}} \left(1 - \frac{\widetilde{d}}{\widetilde{f}_C}\right) > \frac{f_H}{a} \left(1 - \frac{d}{f_C}\right) \tag{S22}$$

See the associated Mathematica notebook for more details.

The exponential model, however, has an associated artefact – the exponential growth of the collective destabilises the internal fixed point before (1,1), in contrast to the logistic model. In Fig. S10, we tracked the independent evolution of Ω_i (panels a,b) and α_i (panels c,d) in a particular system with realistic parameters while numerically checking if feasibility and stability hold throughout evolution. Consider the evolution of obligacies (and similarly for adhesions): Starting from $(\Omega_H, \Omega_S) = (0,0)$, i.e., no dependence, we observe first that both obligacies increase, as expected. However, the trajectory does not reach $(\Omega_H, \Omega_S) = (1,1)$. The obligacies increase to a certain point, making the ecological equilibrium unstable and infeasible. The feasibility bound Eq. (S9) is violated, leading to the collective growth rate becoming too high to sustain equilibrium host/symbiont populations. This barrier in the $\Omega_H - \Omega_S$ plane is artificial due to the unrealistic assumption that the collective population can grow without bound. We therefore "trust" the results of the exponential model only when the traits have low enough values, and in this regime, we can take advantage of the analytics developed above.

Stepping away from the mathematical machinery, there is a clear explanation for the evolution of higher Ω_i and α_i - as a result of the collective's exponential growth, its population grows without bound; so the investment of the host/symbiont in f_C is not unexpected. While this result is, therefore, not surprising in itself, the analytical setup is conducive to asking more nuanced questions.

C. Long-term evolutionary dynamics in the exponential model via the canonical equation. Suppose, for simplicity, that the mutant has obligacy $\widetilde{\Omega}_H$ and the resident has obligacy Ω_i. The invasion fitness is given by

$$s_i(\widetilde{\Omega_i}, \Omega_i) = \tilde{f}_i \left(1 - \frac{d}{\tilde{f}_C}\right) - f_i \left(1 - \frac{d}{f_C}\right).$$

The invasion fitness determines the fate of a given mutant and, therefore, induces a certain path for the evolutionary dynamics of the trait value. This path is given by the canonical equation of adaptive dynamics (38), which is an ordinary differential equation describing the macroevolutionary change, and the obligacy of species i varies as

$$\frac{d\Omega_i}{dt} = \frac{1}{2} \mu_i \nu_i \, x_i^*(\Omega_H, \Omega_S) \frac{\partial s_i(\widetilde{\Omega_i}, \Omega_i)}{\partial \widetilde{\Omega}_i}, \tag{S23}$$

where μ_i, ν_i are respectively the mutation rate and the variance of the mutation step, x_i^* is the equilibrium population size, and the partial derivative is the fitness gradient. By the constraints Eq. (S1) and the fact that $d > f_C$, one sees that the fitness gradient is uniformly positive.

A similar analysis can be accomplished when a mutant has both different obligacy and different adhesion values. Again, tilde-d quantities are associated with the mutant. The invasion fitness is given by

$$s((\widetilde{\Omega}_i, \tilde{\sigma}_i), (\Omega_i, \sigma_i)) = \frac{\tilde{f}_i}{\tilde{a}} \left(1 - \frac{\tilde{d}}{\tilde{f}_C}\right) - \frac{f_i}{a} \left(1 - \frac{d}{f_C}\right).$$

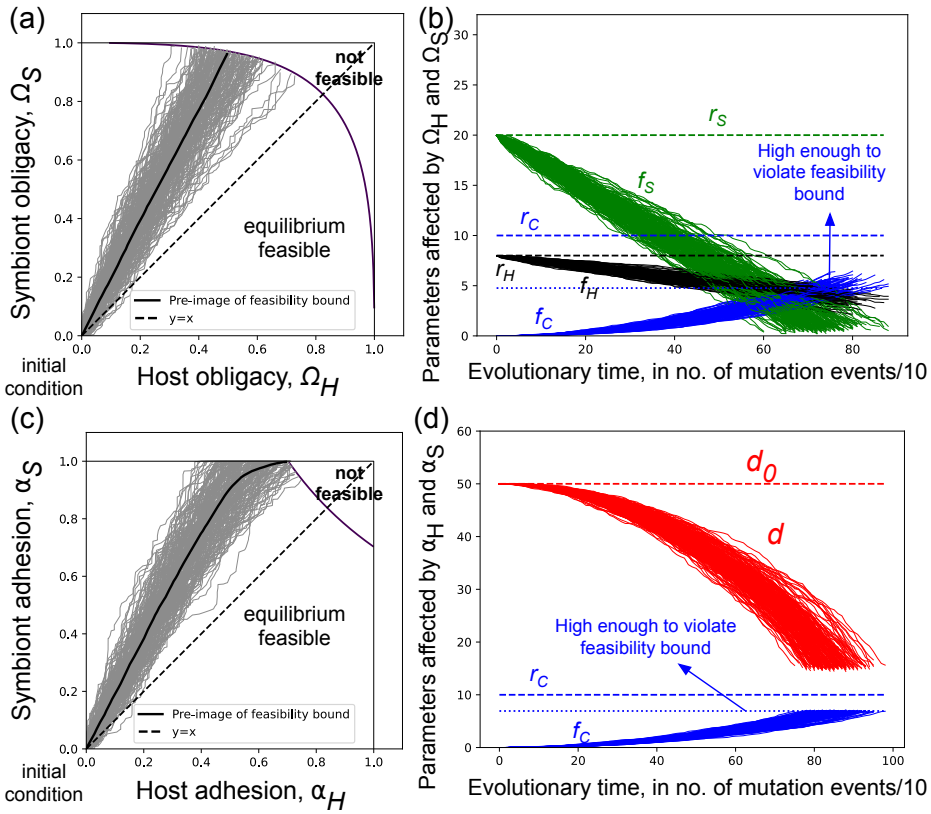

Fig. S10. Evolutionary trajectories are biased towards higher symbiont obligacy. (a,c) For the mappings in Eqs. Eq. (S4) (panels a,b) and Eq. (S5) (panels c,d), we simulated 200 independent evolutionary trajectories. The trajectories monotonically increase with Ω_S (a) and α_S (c) increasing faster respectively, and then stop when the fixed point is no longer stable – this happens precisely at the feasibility bound Eq. (S9). In the infeasible region, the collective population density increases to infinity and, due to dissociation, maintains a comparatively negligible population of independent hosts and symbionts. (See SI §S.5 for information on calculating the average trajectory). **(b,d)** Using the mappings, we can also visualise the dynamics of the growth rates (in a) and the association-dissociation rates (in d). For example, in (b) the independent growth rates decrease, and the collective growth rate increases until it becomes high enough that the feasibility bound is violated. **Parameter values**. (a,b): $r_H = 8, r_S = 20, r_C = 10, K_H = 100, K_S = 200$; for (c,d): $f_H = 8, f_S = 30, r_C = 10, K_H = 100, K_S = 200, a_0 = 0.1, d_0 = 50$.

We write now the canonical equation for a multi (here, two)-dimensional trait:

$$\frac{d(\Omega_i, \alpha_i)}{dt} = \frac{1}{2}\mu_i \;\; x_i^*(\Omega_H, \alpha_H, \Omega_S, \alpha_S)\mathbf{M_i} \cdot \nabla_i s_i((\widetilde{\Omega}_i, \tilde{\alpha}_i), (\Omega_i, \alpha_i)) \,. \tag{S24}$$

Here μ_i is the mutation rate for type i, x_i^* is its equilibrium population size at the given trait values, and $\mathbf{M_i}$ is the variance-covariance matrix of the traits of type i which encodes correlations between these traits. s_i is the invasion fitness for type i, and the gradient is taken with respect to all of its traits. This more general equation is similar in spirit to the earlier equation Eq. (S23), with changes accounting for the now arbitrary (in $\mathbb{N}$) dimension of the trait.
To show that the traits increase, it is sufficient to show that all the entries of $\nabla_i s((\widetilde{\Omega}_i, \tilde{\alpha}_i), (\Omega_i, \alpha_i))$ are positive. Under the constraints on the partial derivatives that we set up initially, and some additional similar constraints on the mapping from traits to ecological parameters, it is straightforward to show this.

D. The impossibility of branching when the invasion fitness is separable. Let $s(y, x)$ be the invasion fitness of a mutant with trait y in the background of a resident population of trait value x, with traits taking value in some set $\mathcal{T}$. We say that $s(\cdot, \cdot)$ is *separable* if there exists a function $\mathcal{F} : \mathcal{T} \to \mathbb{R}_{\geq 0}$ such that one can write $s(y, x) = \mathcal{F}(y) - \mathcal{F}(x)$.
Recall that a mutant invades when its invasion fitness is positive. Therefore, if the invasion fitness is separable, a mutant with trait y invades exactly when $\mathcal{F}(y) > \mathcal{F}(x)$. We notice, then, that an invasion fitness is separable when there is some function $\mathcal{F}(\cdot)$ that acts like a fitness - if y has a higher value of $\mathcal{F}$, then it invades, and if it has a lower value of $\mathcal{F}$ it goes to extinction. Evolutionary trajectories hence maximise this quantity, and therefore, in this sense, the fitness landscape does not change. If

the invasion fitness is separable, one can construct a fitness landscape $\mathcal{F}$ on the trait space such that all permitted trajectories climb up this landscape. Now we prove the observation that we made in the main text regarding the invasion criterion.

Suppose $s(y,x)$ is the invasion fitness describing the evolutionary dynamics of a given system, and that it is separable. Then we will show below that a given strategy x^* is uninvadable if and only if it is convergence stable.

First we define the function

$$G(x) = \left.\frac{\partial s(y,x)}{\partial y}\right|_{y=x}$$

which is the fitness gradient for an invading mutant of trait value y against a resident with trait x. We shall use the fact that for any (C^2) function,

$$\frac{dG(x)}{dx} = \frac{\partial^2 s}{\partial x \partial y} + \frac{\partial^2 s}{\partial y^2}$$

But since s is separable, there is a function $\mathcal{F}$ such that $s(y,x) = \mathcal{F}(y) - \mathcal{F}(x)$. This implies that $\frac{\partial s}{\partial y} = \frac{\partial \mathcal{F}(y)}{\partial y}$ since $\mathcal{F}(x)$ does not depend on y, and then $\frac{\partial^2 s}{\partial x \partial y} = \frac{\partial}{\partial x}\mathcal{F}(y)$ which is obviously zero. So we have shown that

$$\frac{dG(x)}{dx} = \frac{\partial^2 s}{\partial y^2}$$

The left-hand side determines convergence stability, and the right-hand side determines (un)invadability, and since they are equal, these notions cannot diverge!

Recall that a singular strategy is called a branch point, i.e., a point at which evolutionary branching occurs, if it is convergence stable but invadable. A corollary of the above result, then, is that separable invasion fitnesses do not admit branch points - evolutionary branching is impossible. It is perhaps useful to think in terms of the contrapositive: if evolutionary branching is possible, then the invasion fitness is *not* separable.

This is because for a singular strategy to be a branch point, it must by definition be convergence stable but invadable by similar mutants (39). This is possible in general because the conditions to reach a maximum (convergence stability) and to stay there (invadability) are not the same. However, if one can identify a quantity that uniformly increases along all permissible evolutionary trajectories, these notions cannot be different. The reason why is simple and goes as follows. When such a quantity exists, uninvadable points are all convergence stable since they can be reached by trajectories that maximise this quantity. Conversely, convergence stable singular strategies are always uninvadable since any trajectory that converges there must maximise this quantity.

E. Trajectories in the dependence-cohesion plane. In this section, we provide the supporting information for the result that mutual dependence evolves faster than reproductive cohesion. We will first provide an explanation, in terms of the model and then biologically, for why it is adaptive to invest more in obligacy than adhesion. Second, we will show that the bias towards mutual dependence is robust to other minor choices that we made in arriving there.

For providing an explanation, consider the trait-mapping that we have utilised in the main text (Eq. 2 there), also mentioned as Eq. (S3) in this document.

We claimed in the main text that since a change in α_H has the functional effect that depends also on α_S (and vice versa), it has a lesser adaptive benefit than a change in Ω_i. To show this, notice that two important choices were made in arriving at the above trait mapping – first, that the independent growth of the host and symbiont depends only on their own obligacy; second, the dissociation rate depends on both α_H and α_S. However, in general, the independent growth rates can depend on either (i) only their own obligacy or (ii) both obligacies; the dissociation rate can depend on (I) only one adhesion and (II) both adhesions. The “default" map that was motivated by biological reasoning corresponds to the combination i-II above. We shall below give the trait mapping of all other combinations, with each followed by the induced evolutionary trajectories of the traits Ω_i and α_i.

There is another note to be made here: when we make the association and dissociation rates dependent only on one of α_H and α_S, we pick the symbiont trait without loss of generality. This does not have a qualitative effect, and the exact effect will be made clear when necessary. Further, we fix the effect of the obligacies and adhesions on f_C; this does not change because our mental model of an endosymbiosis still stays the same - increasing both of these traits improves collective growth rate. The association rate a will remain a constant here, like in the rest of this work.

In all of the below cases, there will be some commonalities - all four traits always increase, and within each trait pair, the symbiont trait increases faster. This is due to the fact that the exponential growth of the collective and the difference in parameters are not changed over the course of this exercise. The traits increase due to the exponential growth of the collective and the fact that f_C can be increased by any one of the four traits. The symbiont trait increases faster than its corresponding host trait due to the different generation times and carrying capacities.

Now, consider the combination i-I, with results in Figure Eq. (S11). Here, the trait mapping takes the form

$$\begin{aligned} f_H(\Omega_H,\alpha_H,\Omega_S,\alpha_S) &= r_H(1-\Omega_H) \\ f_S(\Omega_H,\alpha_H,\Omega_S,\alpha_S) &= r_S(1-\Omega_S) \\ f_C(\Omega_H,\alpha_H,\Omega_S,\alpha_S) &= r_C\Omega_H\Omega_S\alpha_H\alpha_S \\ d(\Omega_H,\alpha_H,\Omega_S,\alpha_S) &= d_0(1-\alpha_S) \\ a(\Omega_H,\alpha_H,\Omega_S,\alpha_S) &= a \in \mathbb{R}_{\geq 0} \end{aligned} \tag{S25}$$

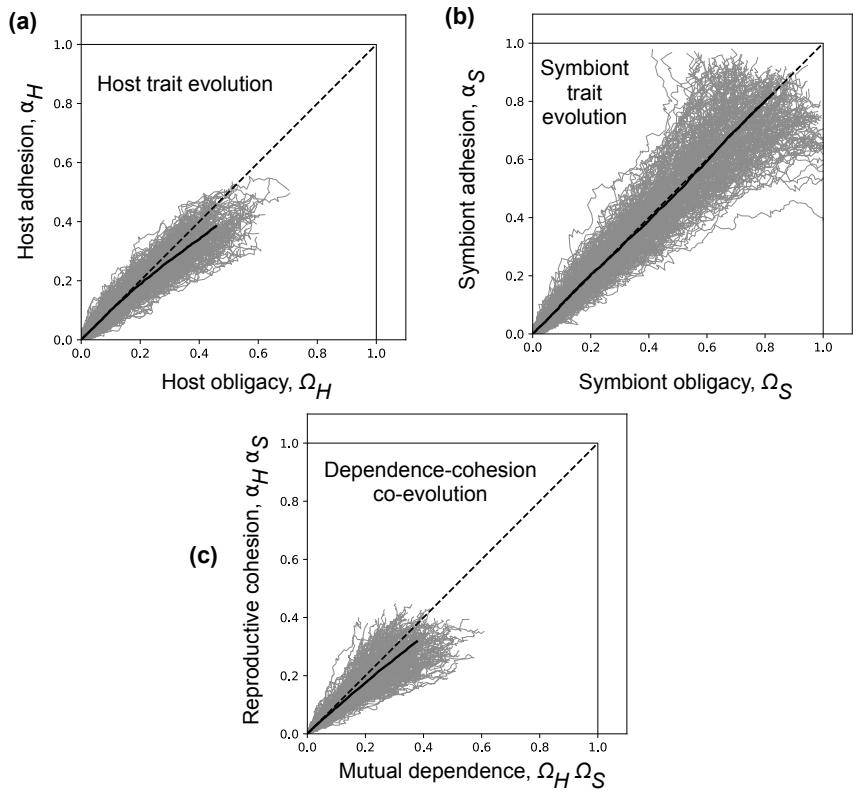

Fig. S11. Independent growth rate depends only on own obligacy, dissociation rate depends only on one adhesion.

Here, there is a slight bias towards mutual dependence, which can be understood by looking at the evolution of the host and symbiont in their own trait space. There is a benefit for both host and symbiont to increase obligacy, and there is the *same* kind of benefit for the symbiont to increase its adhesion since $d = d_0(1-\alpha_S)$. There is a smaller benefit for the host to increase its adhesion because an increased host adhesion only increases f_C but doesn't decrease d. Therefore, Ω_H evolves faster than α_H; however, Ω_S and α_S evolve at the same rate. If instead $d = d_0(1-\alpha_H)$, there is no bias between Ω_H and α_H whereas Ω_S evolves faster than α_S. This leads to a slight bias towards mutual dependence. This bias is a little artificial in the following sense: the bias arises only because we are forced to make a choice between α_H and α_S in the form of d, and would not exist if this choice were not thrust upon us.

Second, consider the combination ii-I with results in Figure Eq. (S12) and the following trait mapping:

$$\begin{aligned} f_H(\Omega_H,\alpha_H,\Omega_S,\alpha_S) &= r_H(1-\Omega_H\Omega_S) \\ f_S(\Omega_H,\alpha_H,\Omega_S,\alpha_S) &= r_S(1-\Omega_H\Omega_S) \\ f_C(\Omega_H,\alpha_H,\Omega_S,\alpha_S) &= r_C\Omega_H\Omega_S\alpha_H\alpha_S \\ d(\Omega_H,\alpha_H,\Omega_S,\alpha_S) &= d_0(1-\alpha_S) \\ a(\Omega_H,\alpha_H,\Omega_S,\alpha_S) &= a \in \mathbb{R}_{\geq 0} \end{aligned} \tag{S26}$$

Here, there is a bias towards reproductive cohesion. This is because the benefit of increasing the adhesion is now stronger than that of increasing obligacy. This is further, to be more precise, because the functional effect of increasing adhesion also does not depend on the other adhesion. There is also a slight bias towards dependence in the host because increasing adhesion for

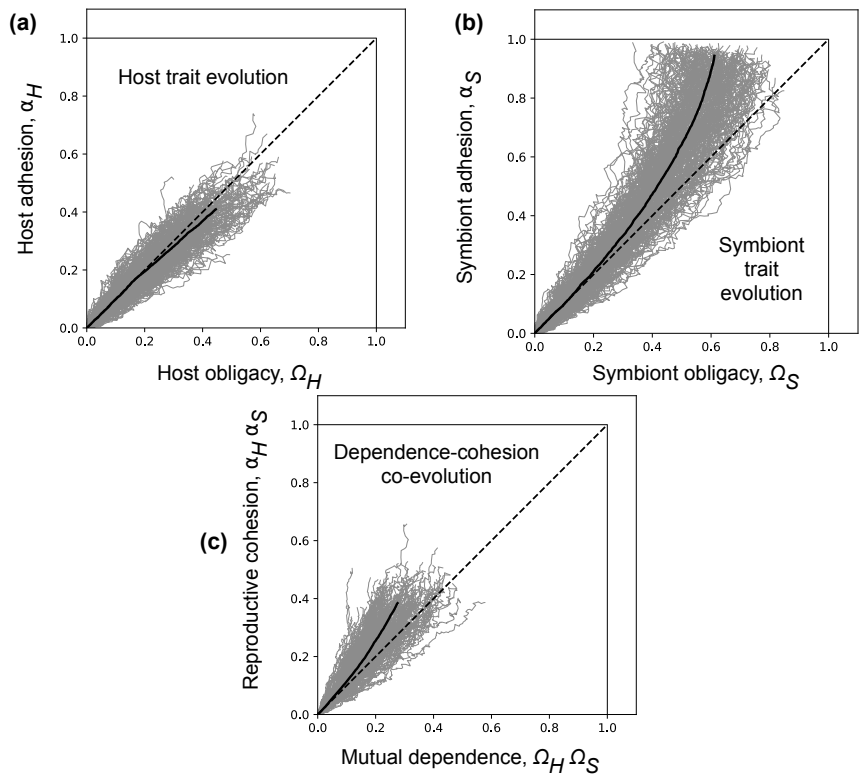

Fig. S12. Independent growth rate depends on both obligacies, dissociation rate depends on only one adhesion.

	i	ii
I	Slight bias	Bias towards reproductive cohesion
II	Default, bias mutual dependence	No bias

Table S1. A schematic description of trajectories in the dependence-cohesion under different kinds of mappings, with the shorthand i-ii-I-II described in Section E. There is a pattern in this table: when both trait pairs Ω_i and α_i combine in the same way to influence ecological parameters (i-I or ii-II), there is little to no bias. The slight bias in i-I case is an artefact, see main text for an explanation. On the other hand, when they combine in different ways (i-II or ii-I), there is a bias towards faster evolution of dependence in one case and faster evolution of cohesion in the other. Our work arrived at case i-II from biological considerations, and we therefore make the associated prediction.

the host does not increase d, but again this is because we are forced to make the same choice between α_H and α_S for d. If instead $d = d_0(1-\alpha_H)$, there would be a slight bias towards dependence in the symbiont and a bias towards cohesion in the host.

Recall that the default combination that we have worked through in the main text is given, in this shorthand, by i-II, so we will not consider it again. Now, lastly, let us study the combination ii-II with results in Figure Eq. (S13) and trait maps:

$$\begin{aligned} f_H(\Omega_H,\alpha_H,\Omega_S,\alpha_S) &= r_H(1-\Omega_H\Omega_S) \\ f_S(\Omega_H,\alpha_H,\Omega_S,\alpha_S) &= r_S(1-\Omega_H\Omega_S) \\ f_C(\Omega_H,\alpha_H,\Omega_S,\alpha_S) &= r_C\Omega_H\Omega_S\alpha_H\alpha_S \\ d(\Omega_H,\alpha_H,\Omega_S,\alpha_S) &= d_0(1-\alpha_H\alpha_S) \\ a(\Omega_H,\alpha_H,\Omega_S,\alpha_S) &= a \in \mathbb{R}_{\geq 0} \end{aligned} \tag{S27}$$

There is, as expected, no bias between mutual dependence and reproductive cohesion. Table S1 summarises the above results.

Now, we shall show that the bias towards mutual dependence is robust to the choices that we made throughout the main text in

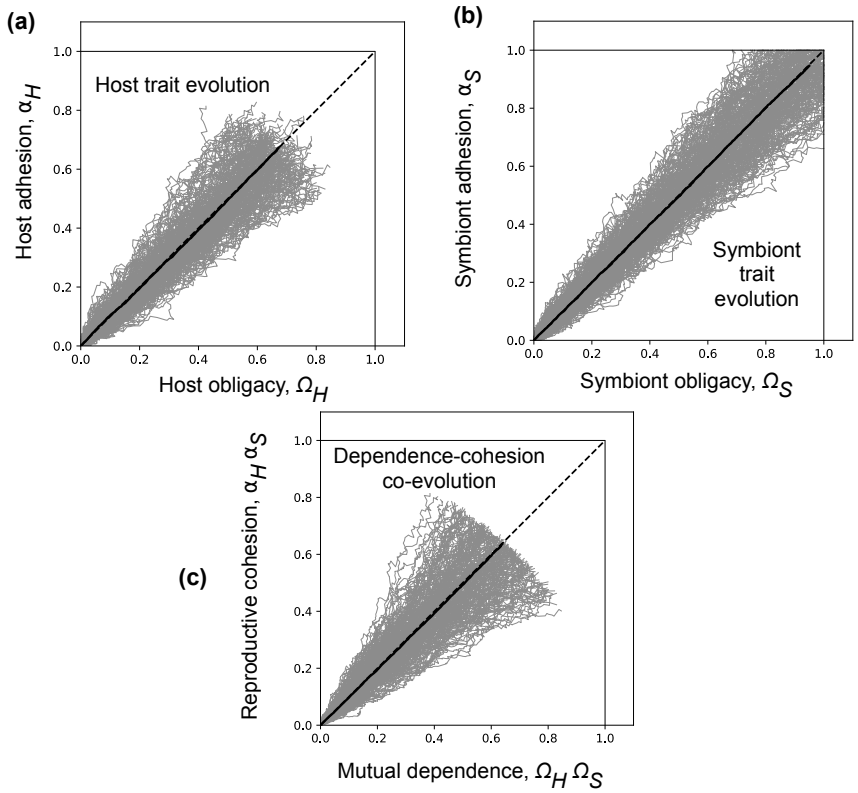

Fig. S13. Independent growth rate depends on both obligacies, dissociation rate depends on both adhesions.

arriving at this result. For ease of reference, we present again the alternate trait map relevant for panel **(a)** of Figure S14

$$
\begin{aligned}
f_H(\Omega_H,\alpha_H,\Omega_S,\alpha_S) &= r_H(1-\Omega_H)\\
f_S(\Omega_H,\alpha_H,\Omega_S,\alpha_S) &= r_S(1-\Omega_S)\\
f_C(\Omega_H,\alpha_H,\Omega_S,\alpha_S) &= r_C\left(\frac{\Omega_H+\Omega_S}{2}\right)\left(\frac{\alpha_H+\alpha_S}{2}\right)\\
d(\Omega_H,\alpha_H,\Omega_S,\alpha_S) &= d_0\left(1-\frac{\alpha_H+\alpha_S}{2}\right)\\
a(\Omega_H,\alpha_H,\Omega_S,\alpha_S) &= a \in \mathbb{R}_{\geq 0}
\end{aligned}
\tag{S28}
$$

Supplementary Note S5: Computation of the average trajectory in simulations with runs of different lengths

Across several figures of the main text and supplementary information, we present plots with several independent simulation runs of different time durations in grey, with a mean trajectory in solid black for interpretational convenience. When our exponential model of population dynamics is involved (Eq. S6), the lengths of these runs might be different. This is because they end when the feasibility boundary (eq. S9) is violated, and this can happen at different times because of the stochasticity of mutant traits. Here we briefly detail how we compute the average trajectory when runs can have different lengths.

Suppose there are N_T total trajectories (grey in the figures). Let L_i be the length of the ith trajectory, and suppose $L_{max} = max_i L_i$ is the duration (hereafter used interchangeably with length) of the longest trajectory, i.e. the trajectory that takes the most time. Denote trajectory i by a function $f_i(t)$ where $t \in \{0,...,L_i\}$ (for example, from zero to the time it takes to reach the feasibility bound). We first artificially extend all trajectories (in time) such that they are all of length L_{max}. In particular, we redefine for each i

$$
f_i(t) = \begin{cases} f_i(t) & 0 \leq t \leq L_i \\ f_i(L_i) & L_i < t \leq L_{max} \end{cases}
$$

Recall that t cannot be larger than L_{max} for any trajectory by definition.

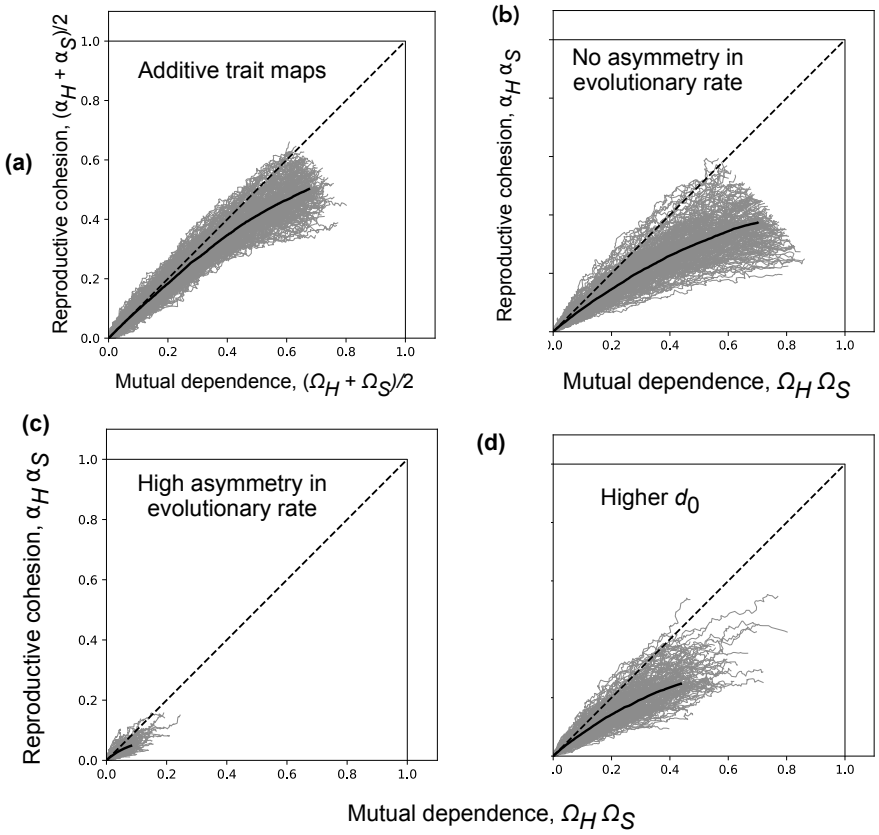

Fig. S14. The bias towards mutual dependence is remarkably robust to model choices. We change important model choices to test the robustness of this result. None of the changes we have made affect its validity. **Base parameter values**. $f_H = 8, f_S = 20, r_C = 10, K_H = 100, K_S = 200, a = 0.1, d_0 = 50$. Changes are made to these values in the text that follows only when explicitly mentioned. **(a)** First, we change the map taking traits to ecological parameters into one where the traits have additive effects: the growth rate of the collective is proportional to the arithmetic mean of Ω_H and Ω_S, etc. The full map is presented in Eq. (E). **(b)** Here, we set $r_H = r_S$ and $C_H = C_S$ while keeping all other parameters fixed. **(c)** Now we set $r_S = 10r_H$ and $C_S = 10C_H$ to understand if a much higher asymmetry in the growth rates and carrying capacities affects evolutionary trajectories. **(c)** Lastly, we set $d_0 = 150$ to understand if a much higher initial dissociation rate does something. It does not, really.

All trajectories are now of the same length, and the mean trajectory $\bar{f}(t)$ (in solid black) is calculated by

$$\bar{f}(t) = \frac{1}{N_T} \sum_{i=1}^{N_T} f_i(t)$$

See the associated GitHub repository for the scripts that this is implemented in.

Supplementary Note S6: A short note for reproducibility

In Figure 3 of the main text, we present the effects of varying the collective carrying capacity K_C and the growth rate scaling parameter r_C. We conclude that r_C does not affect the results, whereas K_C both qualitatively and quantitatively affects the final evolutionary outcomes.

This outcome might sometimes be obscured during reproduction of our results: recall that, during our numerics, instead of the analytically true condition of merely $R_0 > 1$ for the invasion of a mutant, we implement a cutoff of $R_0 > 1 + \varepsilon$ for a small positive value $\varepsilon = 10^{-7}$. This is done to constrain the effects of provably (see Results section) artificial floating point errors which falsely lead to an $R_0 > 1$ at the end of trajectories such as in Figure 2(b,e) of the main text.

However, when r_C is small, the eigenvalues giving rise to the values of R_0 are also very small (smaller than the above $1 + \varepsilon$). When comparing outcomes for different values of K_C, these small R_0 values are not accepted by the condition $R_0 > 1 + \varepsilon$ even though they lead to a systematic increase in the trait values (which can be checked by removing the ϵ).

We impose the criterion $R_0 > 1 + \varepsilon$ for expository clarity, but this criterion can be removed in the associated scripts – it would have the benefit of unambiguous demonstration of the fact that critical K_C values are r_C-independent; but this is accompanied by the cost of artificial fluctuations of trait values even when $R_0 = 1$ which might lead to confusion as well.